JOURNAL OF GEOPHYSICAL RESEARCH, VOL. 95, NO. B12, PAGES 19,583–19,599, NOVEMBER 10, 1990

Volcanic and Tectonic Evolution of the Cascade Volcanic Arc, Central Oregon

GEORGE R. PRIEST

Oregon Department of Geology and Mineral Industries, Portland

From 22 to 0 Ma, σ_3 in the Cascade arc rotated clockwise from approximately N-S to E-W. σ_1 rotated from subhorizontal to vertical at about 7 Ma, producing an extensional stress regime at 7-0 Ma. Rotation of σ_1 and σ_3 was likely a response to decreasing influence of ENE to NE compression at the Juan de Fuca plate-North American plate (JDFP-NAP) boundary relative to N-S compression and attendant continental extension produced at the Pacific plate (PP)-North American plate boundary. Decreases in orthogonal convergence rate, convergence angle, and length of the convergent margin relative to the NAP-PP transform boundary caused the stress rotations. Volcanic production decreased by a factor of 3 from the interval 35-17 Ma to 16.9-7.4 Ma, probably reflecting a decrease in convergence rate. Volcanic production increased at 7.4-0 Ma even though convergence rate continued to decrease. The extensional stress regime at 7-0 Ma promoted mafic volcanism that caused the increased volcanic production. Volcanic production is therefore a function of convergence rate and upper plate stress regime. The volcanic front migrated progressively eastward from 35 to 0 Ma as the volcanic belt narrowed. The narrowing was caused primarily by steepening slab dip at depths greater than 100 km. Eastward migration was likely caused by decreasing shallow (0-100 km) slab dip resulting from thinning of the NAP. Uplift of the Western Cascades province in the early Pliocene may have been caused by vigorous flow into the mantle wedge accommodating an increase of free rollback rate of the subducted plate at 4 Ma.

INTRODUCTION

Volcanic arcs around the Pacific basin are now universally thought to be the product of partial melting events caused by the subduction of oceanic lithosphere. Many of these volcanic arcs have features in common with the Cascades arc; these include an inactive volcanic arc seaward of an active arc (e.g., Mariana arc; review by *Dickinson* [1973]), a history punctuated by periods of uplift and deformation (e.g., Andean arc), and progressive changes in the relative and absolute eruption rates of mafic, intermediate, and silicic volcanic rocks (e.g., Fiji; review by *Gill* [1981]).

The central Oregon Cascades is an ideal natural laboratory to study these phenomena because the arc there is landward of a relatively simple part of the subduction zone free of the complicated motions attributed to segments of the Juan de Fuca plate at its north and south ends (Figure 1) [*Riddihough*, 1984].

The geologic evolution of the Cascades between 44°N and 44°52′30″N (Figure 1) will be examined with the aim of understanding the processes responsible for the above features. I will show that these phenomena are most likely controlled either directly or indirectly by the absolute and relative motions of the major plates.

LITHOLOGIC NOMENCLATURE

Rock names are assigned according to the system of *Taylor* [1987], based on analyses recalculated to 100% totals, volatile-free. The term "tholeiitic" is used to designate rocks with high Fe/Mg and high Fe contents, plotting in the tholeiitic fields of *Miyashiro*'s [1974] FeO^*/MgO versus SiO_2 diagram and *Irvine and Baragar*'s [1971] alkalis-femic oxides-MgO (AFM) diagram. The term "calc-alkaline" refers to rocks that plot in the calc-alkaline fields of the these two diagrams. The term "silicic" refers collectively to dacite and rhyodacite. The term "mafic" is used for basalt, basaltic andesite, and tholeiitic andesite. Tholeiitic andesite is included in the mafic rocks, because (1) tholeiitic andesite is lithologically similar to basalt and basaltic andesite, containing an abundance of dark colored ferromagnesian minerals, and (2) the term mafic refers to enrichment in dark colored ferromagnesian minerals [e.g., *Bates and Jackson*, 1980].

Paper number 90JB01393.
0148-0227/90/90JB-01393$05.00

STRATIGRAPHIC NOMENCLATURE

This paper will deal with five time-rock "episodes" that are marked by rocks and unconformities that can be recognized throughout the study area with minimal support from isotopic age data. The episodes are episode 1 (35-17.0 Ma), 2 (16.9-7.5 Ma), 3 (7.4-4.0 Ma), 4 (3.9-0.731 Ma), and 5 (0.730-0 Ma). Relationships to regional rock-stratigraphic and time-rock units are shown in Figure 2.

RADIOMETRIC AGE DATA

Isotopic age data (Figure 3) are taken from compilations by *Fiebelkorn et al.* [1983], *Hammond et al.* [1980], and *Walker and Duncan* [1989], modified by data from *Priest et al.* [1987*b*, 1988, 1989] and *Black et al.* [1987] and the data of Table 1. Ages were determined primarily with the K-Ar and ^{40}Ar-^{39}Ar techniques, although one fission track age [*Hammond et al.*, 1980] and one U-Pb age [*Priest et al.*, 1989] are also included. These K-Ar ages were excluded, owing to probable argon loss caused by alteration of the samples. Three ages were excluded because stratigraphic relations and other age data on the same units indicate grossly different ages. Age data from one sample were excluded because of uncertainties about its location (published location is on a landslide).

GEOLOGIC HISTORY OF THE CENTRAL OREGON CASCADES

Introduction

The geologic history and structure were interpreted from geological compilation maps and cross sections (Figures 3-6). Geologic data are based on a scale 1:250,000 geologic map produced from previous compilations [*Walker and Duncan, 1989*; *Sherrod and Smith*, 1989] augmented by my reconnaissance mapping in 1988

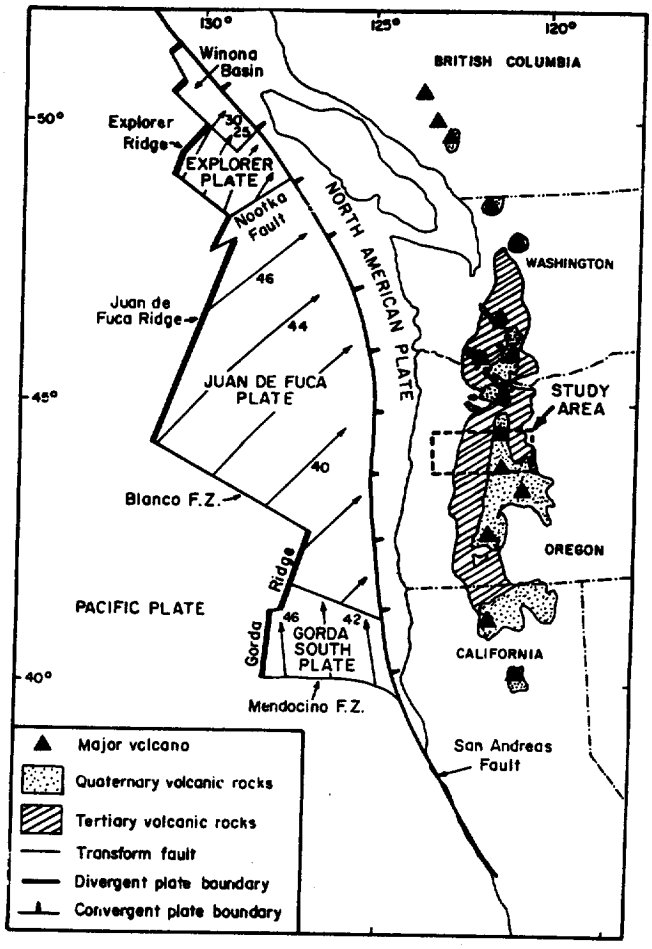

Fig. 1. Plate tectonic map of the northwestern American continent showing major crustal boundaries, the Cascade volcanic arc, and location of the study area. Arrows show the net vectors in kilometers per million years of Juan de Fuca plate motion relative to the North American plate. Figure modified from *Riddihough* [1984], *McBirney* [1968], and *Sherrod and Smith* [this issue].

and by detailed mapping of *Priest et al.* [1987*b*, 1988], *Black et al.* [1987], and *Niem et al.* [1987].

Details of the geologic history of the volcanic arc are discussed by *Taylor* [1981, this issue], *Priest et al.* [1983], and *Priest* [1989].

		Ma	THIS PAPER EPISODES	PRIEST AND OTHERS (1983) EPISODES	PECK AND OTHERS (1964)
Quaternary		0.73	5	Late High Cascades	High Cascade Volcanic Rocks
Tertiary	Pliocene	4	4		
	Miocene	7.4	3	Early High Cascade	
		17	2	Late Western Cascade	Sardine Fm.
	Oligocene		1	Early Western Cascade	Little Butte Volcanic Series
	Eocene	35			?—?—?—?—

Fig. 2. Correlation of volcanic episodes and regional rock units.

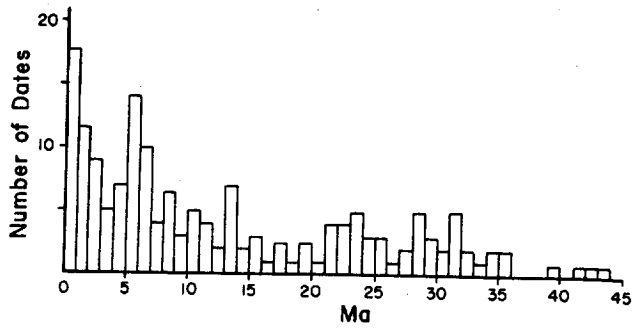

Fig. 3. Histogram of isotopic age data taken from *Black et al.* [1987], *Fiebelkorn et al.* [1983], *Hammond et al.* [1980], *Power et al.* [1981], *Priest et al.* [1987*b*, 1988], *Verplanck* [1985], *Walker and Duncan* [1989], five new K-Ar ages (Table 1), and one U-Pb age [*Priest et al.*, 1989].

The following is in large part a summary of those observations.

35-17 Ma: Early Western Cascade Volcanism (Episode 1)

Early Western Cascade volcanism probably began at about 35 Ma. Local andesitic volcanos and voluminous eruptions of tholeiitic lava and silicic pyroclastic rock characterized the volcanism. The active volcanic belt was probably 3-4 times the width of the Quaternary arc. The lateral continuity of ash flow sheets indicates that the arc was relatively low in elevation, particularly in the early part of the episode, when it was almost certainly a subsiding basin. The strandline of a Pacific embayment was located at or within a few km the volcanic front [*Snavely and Wagner*, 1963; *Orr and Miller*, 1984].

A period of deformation occurred sometime before about 25 Ma, tilting and faulting rocks (unit 1a, Figure 5) in the north central part of the study area at the Breitenbush anticline and Hoover fault zone (Figure 6). Voluminous eruptions of ash flow tuff and subordinate tholeiitic lava followed the main period of deformation (unit 1b, Figure 5). The Breitenbush anticline (Figure 6) is formed from juxtaposition at the Hoover fault zone of the east dipping episode 1 and 2 rocks on the east side of the Western Cascades province against the rocks tilted northwest prior to 25 Ma (Figures 4-6). This complex structure has been interpreted as evidence of folding at 18-12 Ma [*Sherrod and Conrey*, 1988] but may in fact be the product of multiple deformational events in an area of oblique-slip faulting [*Priest et al.*, 1987*b*].

16.9-7.5 Ma: Late Western Cascade Volcanism (Episode 2)

Early Western Cascade volcanism ended with a period of uplift or low volcanic activity that lasted from about 18 Ma to about 14 Ma, producing a marked unconformity between episode 1 and 2 rocks in most areas. At 15.3 Ma [*Lux*, 1982] lavas of the Columbia River Basalt Group flowed into northwestern Oregon, including a lowland now occupied by the Willamette Valley (Figure 6). The southern part of the Valley is a strike valley eroded in east tilted rocks that are partly covered by the Columbia River Basalt Group [*Sherrod and Pickthorn*, 1989]. The east tilting of 5°-10° (Figure 6) must therefore have occurred prior to 15.3 Ma.

Eruption of dacitic ash flows and air falls of the late Western Cascade episode began at about 14 Ma, but even more voluminous eruptions of calc-alkaline two-pyroxene andesite and subordinate basaltic andesite and dacite dominated volcanism from about 13 to 8.8 Ma.

The episode 2 rocks dip gently eastward in much of the eastern part of the Western Cascades province. However, instead of "skying out" over the western part of the Western Cascades, the rocks crop out at the tops of many western ridges (Figures 4 and 5), suggesting that these eastward dips roll over westward to sub-

TABLE 1. New K-Ar Data

Drill Hole[a]	Sample[b]	K[c], wt %	Radiogenic $^{40}Ar^{c}$, mol/gx10^{-12}	Radiogenic $^{40}Ar^{c}$, %	Material Dated	Rock Type	Longitude W	Latitude N	Elevation, m	Age, Ma
82-4	88-4-810	0.734	0.093	0.3	Plagioclase	basalt	121°41.53′	44°13.73′	1219	0.073±0.034[d]
83-2	88-2-1819	1.037	0.262	1.0	Plagioclase	basalt	121°45.87′	44° 2.12′	1110	0.15±0.05[d]
[illegible][e]	PP-2	0.56	0.54	8.3	Plagioclase	basalt	121°59.88′	44°41.33′	616	0.54±0.05
82-3	88-3-1240	0.349	0.816	1.2	Plagioclase	basalt	121°43.30′	44°33.90′	896	1.35±0.07[d]
82-3	88-3-1741	0.273	0.705	0.6	Plagioclase	basalt	121°43.30′	44°33.90′	743	1.49±0.06[d]

[a] Analyses by P.E. Damon and M. Shafiquallah, University of Arizona.
[b] Number of Unocal diamond core hole.
[c] Last number on drill hole sample numbers is the depth in feet.
[d] Mean value.
[e] Age and location from *Priest et al.*
[f] Not applicable.

horizontal or gently west dipping. The outcrop pattern and measured dips in episode 2 rocks [*Walker and Duncan*, 1989] support this interpretation. However, *Sherrod and Pickthorn* [1989], working in the Western Cascades at latitudes 43°-44°N, found similar eastward dips in both episode 1 and 2 rocks, concluding that east tilting occurred after 12 Ma. It may be that south of 44°N structural history changes or that preservation of episode 2 rocks in the western part of the Western Cascades is not good enough to demonstrate the westerly dip of the sequence. The latter possibility is suggested by the increasingly poor preservation of episode 2 rocks from north to south in the western part of the study area (Figure 4). Preservation of a small area of episode 2 rocks at 43°50′N in the westernmost part of the Western Cascades [*Woller and Priest*, 1983] demonstrates that the easterly dip of the sequence noted in areas to the east [*Woller and Black*, 1983] does not continue westward at that latitude.

The extent and volume of the episode 2 volcanos are difficult to reconstruct, because later erosion has removed much of the

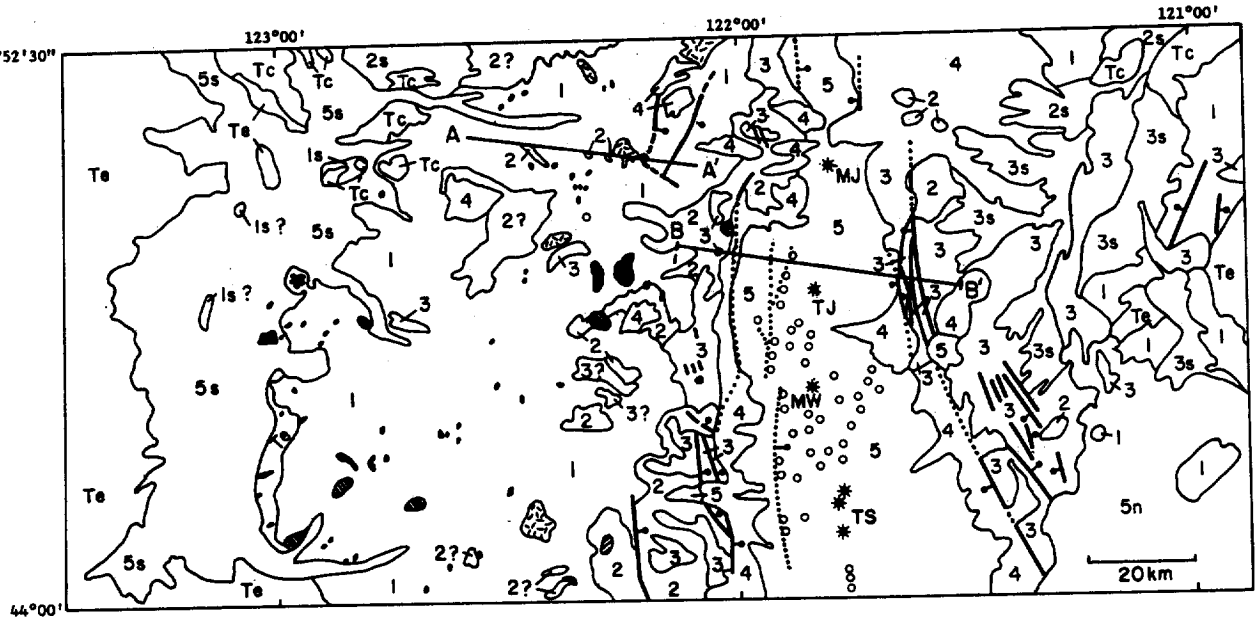

Fig. 4. Generalized geologic map of the study area modified from *Walker and Duncan* [1989] and *Sherrod and Smith* [1989] (see text for explanation of modifications). This map is a generalized version of a more detailed scale 1:250,000 map utilized for interpretations of volcanic volume and geologic history.

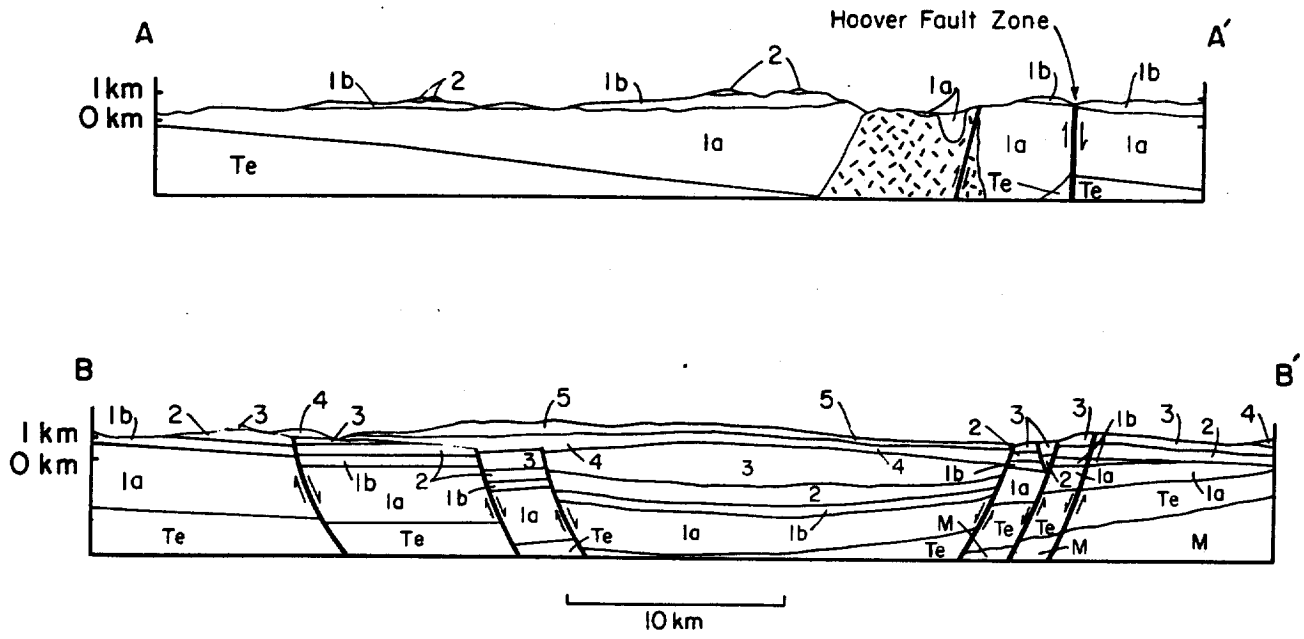

Fig. 5. Cross sections A-A′ and B-B′ of the geologic map (Figure 4). Note that episode 1 rocks aged 35 to >25 Ma and 25 to 17 Ma are labeled 1a and 1b, respectively. Unit M is Mesozoic rock. All other unit labels are defined in Figure 4.

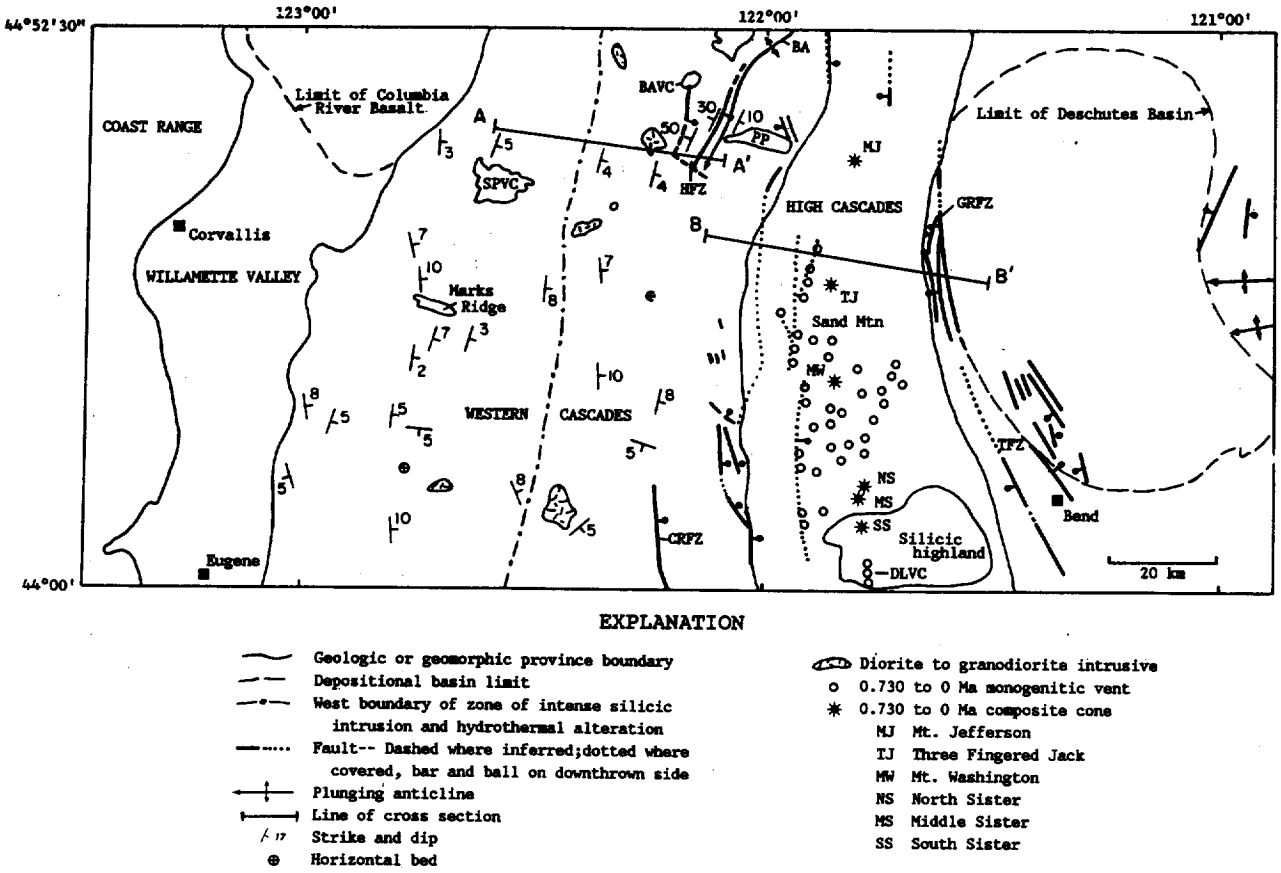

Fig. 6. Tectonic and physiographic map of the study area. Labels are as follows: SPVC, Snow Peak volcanic center; BAVC, Battle Ax volcanic center; MJ, Mount Jefferson; TJ, Three Fingered Jack; MW, Mount Washington; NS, North Sister; MS, Middle Sister; SS, South Sister; DLVC, Devils Lake volcanic center; BA, Breitenbush anticline; HFZ, Hoover Fault Zone; CRFZ, Cougar Reservoir Fault Zone; GRFZ, Green Ridge Fault Zone; TFZ, Tumalo Fault Zone; PP, Pigeon Prairie. The limit of the Deschutes Basin is taken from *Smith* [1986].

volcanic material. The sequence is near the top of the Western Cascade mountains, so it has been particularly vulnerable to erosion accompanying uplift of the area during the early Pliocene. Erosion was accelerated by the tendency of basal nonwelded ash flow and air fall tuff to act as a slip plane for landslides.

Tephra was also not efficiently trapped during the volcanism, because there was probably not a subsiding basin. This interpretation is supported by the high (50-700 m) relief on local unconformities within the sequence and limited areal extent of ash flow tuff units [e.g., *Priest and Woller*, 1983*a*; *Priest et al.*, 1988].

In spite of the extensive erosion, thick sections of episode 2 rock are locally well preserved where the sequence is draped over the east dipping episode 1 rocks in the eastern and northwestern part of the Western Cascades province (Figure 4). For example, isotopic age data suggest that the entire section is preserved near the Cougar Reservoir Fault Zone (Figure 6) [*Priest et al.*, 1988]. These well-preserved sections were used to estimate thicknesses for estimates of volcanic production.

Andesitic intrusions and thick flows of andesite and dacite are probably at or close to vents in the eastern part of the Western Cascades province (Figures 3 and 4). There is also a large hornblende andesite volcano of episode 2 that emerges from the cover of younger rocks on the east side of the High Cascades province [*Hales*, 1975] (outcrop east of Mount Jefferson, Figure 4). Therefore the minimum width of the volcanic arc was probably about 60 km, narrower than the episode 1 arc but wider than episode 3-5 arcs.

7.4-4.0 Ma: Early High Cascade Volcanism (Episode 3)

Eruptions of basalt and basaltic andesite began at 7.4 Ma centered on a volcanic axis essentially coincident with the current High Cascade axis [*Taylor*, 1981; *Smith et al.*, 1987]. This early High Cascade volcanism, episode 3, was characterized by eruption of voluminous basalt, basaltic andesite, and subordinate silicic ash flows and air falls.

The volcanic arc was about 13 km wider than the modern High Cascade arc and is now largely hidden from view, owing to subsidence into graben structures that ended the episode at about 5.4-4 Ma [*Taylor*, 1981; *Smith et al.*, 1987; *Priest et al.*, 1988]. This arc width is probably not significantly modified by later extension, because total extension on normal faults inferred on cross section A-A′ (Figure 5) is less than 1 km. However, extension taken up by magmatic intrusion without faulting is unknown and may be significant.

Uplift of the Western Cascades

The Western Cascades province was uplifted in the early Pliocene at about the same time that much of the High Cascades was subsiding into grabens [*Williams*, 1953; *Priest et al.*, 1983; *Sherrod*, 1986]. The best evidence of uplift is the regional entrenchment of streams. The largest rivers, the North Santiam and McKenzie River, have about 1 km of relief in the eastern part of the Western Cascades, decreasing to essentially no relief at the Willamette Valley. The youngest volcanic rocks at the tops of the uplifted ridges have ages of 4.5 ± 0.3 Ma (Marks Ridge, Figure 6) [*Verplanck*, 1985] to 5.13 ± 0.01 Ma [*Priest et al.*, 1988]; younger volcanic rocks are generally intracanyon lava flows. These observations suggest but do not prove that the Western Cascades were uplifted some time after 5 Ma. Stream entrenchment might also have been caused by changes in base level outside of the Western Cascades province.

The entrenchment of streams in the Western Cascades cannot be explained by lowering of sea level, because (1) there is no evidence that sea level has changed by large enough amounts, and (2) the sea has been absent from the mouths of Western Cascade streams since the early Miocene [*Snavely and Wagner*, 1963; *Orr and Miller*, 1984]. Only local base levels controlled by master streams in the Willamette Valley or intra-arc graben have any significance for Western Cascade rivers.

Formation of intra-arc graben in the High Cascades at 5.4 Ma [*Smith et al.*, 1987], cannot account for stream entrenchment in the Western Cascades, because streams not connected to grabens were rejuvenated. For example, intracanyon lava flows of the Battle Ax volcanic center (BAVC, Figure 6) followed 2 Ma streams that were incised 600-900 m in episode 1 rocks [*Thayer*, 1939; *White*, 1980; *Priest et al.*, 1987*b*]. Lava flows from the Snow Peak volcanic center (SPVC, Figure 6) filled 3 Ma valleys [*Verplanck*, 1985] with 670 m of relief [*Peck et al.*, 1964]. Lavas and sediments were still being trapped in the graben at 1.8-1.9 Ma [*Black et al.*, 1987; *Priest et al.*, 1988], so west flowing Western Cascade rivers had not yet established a connection to the graben when stream incision was far advanced in the Western Cascades.

There is no evidence that the Willamette Valley has undergone post-5 Ma subsidence sufficient to cause 1 km of stream incision in the Cascades. The valley has probably been at low elevation since lava of the Columbia River Basalt Group (CRBG) flowed into the area at 15.3 Ma [*Lux*, 1982; *Beeson and Tolan*, this issue]. Individual basalt flows of CRBG cover hundreds of square kilometers of the Valley and source areas to the east, indicating deposition on surfaces of low gradient and relief that were not far above sea level [*Beeson and Tolan*, this issue]. The base of the 150-m-thick CRBG still lies close to sea level at the Valley axis [*Beaulieu et al.*, 1974], so there is no evidence that large changes in elevation have occurred.

There is also no evidence that the Willmette Valley has been incised deeply enough to produce the Western Cascade stream incision. Post-15.3 Ma erosion has locally cut through the CRBG, but the Willamette River now meanders across a fill of Plio-Pleistocene to upper Pleistocene sediments [*Niem et al.*, 1987] at 60-90 m above sea level. The maximum depth of this fill is between 80 m [*Niem et al.*, 1987] and 150 m (W.A. Niem, personal communication, 1989). Therefore less than 240 m of erosion occurred in the Willamette Valley between 15.3 Ma and the Pleistocene.

Uplift is not the likely cause for most of this erosion in the Willamette Valley. Streams probably began to cut through the 150 m of ponded CRBG soon after deposition, responding to a disrupted stream gradient. The less than 90 m of erosion below the CRBG might be from uplift, but, if so, the elevation of the erosional surface holding the Plio-Pleistocene sediments (below current sea level) suggests that the absolute uplift was relatively minor. The Pliocene stream incision in the Western Cascades was therefore probably caused by an uplift that did not affect the Willamette Valley.

Was uplift of the Western Cascades abrupt or gradual? *Sherrod* [1986] presents evidence from 6 to 30 km south of the study area that suggests that rapid uplift occurred there between 5-6 Ma and 3.3 Ma. He utilized stream profiles based on intracanyon lava flows and present stream gradients to show that gradients rapidly decreased from 3.3 to 2 Ma, then decreased much more slowly from 2 Ma to present. Similarity of *Sherrod*'s [1986] stream incision rates to those in this study area [e.g., *Priest et al.*, 1988] suggests that the two areas experienced similar rates of uplift.

3.9-0 Ma: Late High Cascade Volcanism (Episodes 4 and 5)

Whereas late High Cascade volcanism at 3.9-0 Ma was compositionally identical to episode 3, eruptions occurred from a narrower volcanic arc confined on the west by the uplifted Western Cascades and partially confined on the east by west facing fault scarps (e.g., Green Ridge, Figure 6). Upper Pliocene and Quaternary intracanyon flows and volcanic centers do occur in the Western Cascades province, but they are rare (Figure 4).

The late High Cascade episode is separated into two episodes (episodes 4 and 5) at 0.730 Ma, the beginning of the Brunhes normal magnetic polarity epoch. This division was adopted primarily for use in calculations of volcanic production, taking advantage of mapping by *Sherrod and Smith* [1989] in the High Cascades.

However, the division has also some geologic significance. Volcanic rocks older than about 0.730 Ma are generally in poorly preserved volcanic landforms and along intracanyon benches perched on the sides of younger valleys. Volcanic rocks younger than this are generally from well preserved volcanic landforms with intracanyon flows exposed at the bottom of modern valleys.

CHANGES IN VOLCANIC PRODUCTION RATE

Introduction

Volcanic production rate changed dramatically during the last 35 m.y. in the Cascades. Correlation of rate changes to the tectonic events may provide insight into causative mechanisms.

Calculation Method

Volcanic production rates (R_v) were calculated as follows:

1. A scale 1:250,000 map was constructed of the preerosion distribution of all time-rock units by smoothly connecting westernmost and easternmost outcrops of volcanic rock (generalized version shown in Figure 7). No attempt has been made to estimate the total extent of epiclastic rocks fringing the arc, although the thickest part of the debris aprons adjacent to the arc were included where sufficiently well preserved to be estimated. Gentle eastward dip of episode 1 and 2 rocks in many areas causes the western part of these sequences to be eroded off, making reconstruction of the preerosion extent highly uncertain. The westward extent for rocks of both of these episodes was arbitrarily set at the westwardmost outcrop. The western boundary was then drawn approximately parallel to the north-south trend of the arc. The eastward extent of episode 1 volcaniclastic rocks extends outside the study area and was arbitrarily set at the east boundary of the study area.

2. The area of each time-rock unit was measured utilizing a planimeter. The areas were tabulated separately for the rectangular areas illustrated in Figure 7. The size, particularly the east-west width, of the rectangular areas was adjusted to minimize variations of stratigraphic thickness within each.

3. Total thickness of each time-rock unit was determined from geological cross sections of each rectangular area of Figure 7. Thickness varies significantly from east to west across most grid areas, and in those cases an average value was determined by inspection. Little variation in thickness was noted north to south within each grid area. If insufficient data were available in a grid area to construct a cross section useful for estimation of a thickness, thickness data from the adjacent grid area to the north or south were utilized. This problem was mainly an issue for the three grid areas in the south central part of the map where the thickness of covered episode 1 rocks was estimated from inferences based on rocks exposed by the Hoover Fault Zone to the north (Figure 6).

4. Thicknesses of episode 1 and 2 rocks under the cover of younger rocks in the central part of the map were inferred by assuming (1) that the maximum thickness occurs at the same longitude as the maximum exposed thicknesses in the Western Cascades province, and (2) that the thickness decreases smoothly eastward to the thickness of exposures east of the younger rocks.

5. Where rocks have significant dips, average thickness was calculated for rocks exposed within the grid area. No attempt was made to estimate how much rock might have been eroded off a grid area. Whereas this method systematically underestimates the total thickness of rocks with significant dip, it is more reproducible than estimating cross-sectional shapes of the preerosion volcanic piles. The shapes probably varied radically from episode to episode, depending on the ratio of lavas to clastic rocks, rate of subsidence, rate of volcanic arc migration, and deformation. This problem was mainly an issue for east dipping rocks of episode 1 exposed in the two westernmost grid areas.

6. The average thickness of mafic, andesitic, and silicic rocks

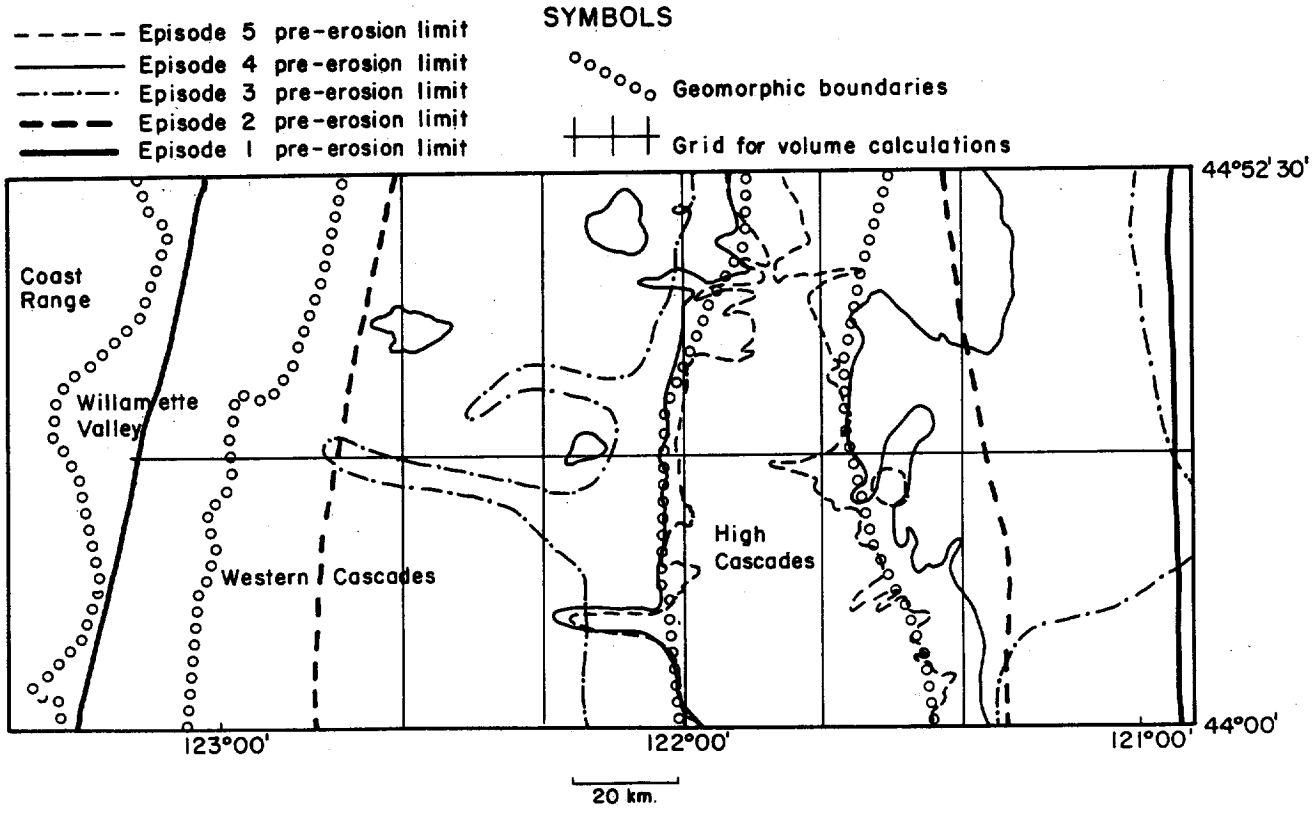

Fig. 7. Shows inferred original extent of rocks of each episode before erosion. Grid lines show areas for which an average thickness of each unit was inferred for volume calculations.

was estimated from detailed traverses in representative areas and measurement of the areal frequency of outcrops of various rock types. In the case of volcaniclastic sequences, the relative amounts of mafic, andesitic, and silicic rocks in lithic clasts was crudely estimated from thin sections and from random sampling of pebble- to cobble-size clasts in a few representative areas. The relative amount of vitric and lithic clasts was estimated from direct field tabulations of well-exposed, representative sections. These relative amounts were then taken as proportions of the thickness of the volcaniclastic units and added to the other average thickness estimates.

7. Volume (Table 2) was calculated for each grid area by multiplying the average thickness by the area, yielding a "brick-shaped" volume. Volumes were not reduced to dense magma equivalents. Volumes for composite cones of episode 5 rock were tabulated separately from the shield-like platform of Quaternary rocks. Volumes of cones were calculated assuming a perfect cone shape with a flat base sitting on the platform rocks.

8. R_v (Table 3) was calculated by dividing the total volume of each rock composition by the span of geologic time and length of the volcanic arc between 44°N and 44°52′30″N.

Error Analysis

Uncertainties in rate estimates arise mostly from two factors. First, the estimate of average thickness of each unit is subjective and highly sensitive to the amount of detailed map data. Second, the amount of each unit lost to erosion is unknown, particularly in dipping sequences of episode 1. The second factor is the most important, systematically underestimating the quantity of older rocks.

The large amount of ash lost through wind dispersal is a major factor for episode 1, which is characterized by numerous explosive eruptions. The chemistry of thick air fall ash deposits of the John Day Formation of eastern Oregon is consistent with an origin in the episode 1 arc [*Robinson and Brem*, 1981]. Estimation of the volume of Cascade ash in the John Day Formation is beyond the scope of this paper, but it is likely that addition of this rock would increase the calculated volcanic rate for episode 1 by about 25%. Likewise, the east dipping volcaniclastic units of episode 1 that have been eroded off of the westernmost grid areas probably account for a similar amount. Therefore the calculated volume of episode 1 rock is probably only about 60-70% of the actual volume.

The volume of tephra lost to erosion is heavily dependent on whether a basin of deposition was available to catch sediments. Preservation of thick sections of volcaniclastic rock in episode 1 suggests that a subsiding basin was available at that time, but widespread unconformities and disconformities between and within the episodes illustrate that such basins did not persist. For example, ash flows, debris flows, and hyperconcentrated flood flows probably spilled east and west off of the episode 3 arc, but these volcaniclastic rocks are in general preserved only in an eastside basin [*Smith*, 1987]. There is no evidence that a basin was in existence during episode 2.

Uncertainty in elapsed time applicable to each volume of rock was generally not a major source of error, except for episode 1. Basal ages of episode 1 rocks tend to cluster at about 30-35 Ma with a few K-Ar ages as old as 40-43 Ma (Figure 3). *Walker and Duncan* [1989] argue for an age of 32-17 Ma for rocks of episode 1; however, assuming no repeat of the section by faulting, there is about 1300 m of episode 1 rock below an ash flow tuff that they dated at 32.1 Ma. They also show an age of 30.1 Ma near the base of the section in the southern part of the study area. I prefer a basal age of 35 Ma, the high-quality K-Ar age from an ash flow tuff at the basal contact of the Cascade section 75 km south of the study area [*Smith et al.*, 1980]. Rate estimates are given for the total range of isotopic ages (43-17 Ma) and for the preferred range of 35-17 Ma (Table 3).

Comparison With Other Rate Estimates

Rates of volcanic production reported here were similar in many respects to previously reported rates. I found the same decrease in volcanic production from the Oligocene to the middle Miocene noted by *Verplanck and Duncan* [1987]. I also agree with the finding of *McBirney et al.* [1974] that basalt and basaltic andesite are the dominate rocks in Pliocene and Quaternary sequences.

There are also some notable differences between my volcanic production rates and those of other workers. I found that one of the lowest rates was in the middle Miocene, whereas higher rates prevailed before and after. *McBirney et al.* [1974] inferred that the highest rates were in the middle Miocene. I also did not find andesite to be a particularly abundant eruptive product overall, whereas andesite dominates the early history of arc, according to *McBirney et al.* [1974]. These differences stem mainly from use here of more detailed map and age data and a smaller study

TABLE 2. Volcanic Rock Volumes

Rock Type	43.2(35)[a]-17.5 Ma	16.9-7.5 Ma	7.4-4.0 Ma	3.9-0.731 Ma	0.730-0 Ma
Mafic	12,316	1,106	4,046	2,541	733
Andesitic	3,929	4,461	4	316	36
Silicic	20,639	865	935	222	118
Total	35,882	6,432	4,984	3,079	887

Values in cubic kilometers.
[a] Volume probably mostly from 35-17 Ma rocks.

TABLE 3. Volcanic Production Rate R_v

Rock Type	43.2-17 Ma	35-17[a] Ma	16.9-7.5 Ma	7.4-4.0 Ma	3.9-0.731 Ma	0.730-0 Ma
Mafic	4.8	7.0	1.2	12.1	8.2	10.2
Andesitic	1.5	2.2	4.8	0	1.0	0.5
Silicic	8.0	11.7	0.9	2.8	0.7	1.6
Total	14.3	20.9	6.9	14.9	9.9	12.3

Values in km^3 $m.y.^{-1}$ (km arc length)$^{-1}$.
[a] Preferred R_v (see Table 2 and text).

area. I also lumped iron-rich (tholeiitic) andesites of episode 1 with the mafic rocks, whereas previous workers did not generally recognize the iron-rich nature of these rocks, lumping them with calc-alkaline andesites or basaltic andesites. Tholeiitic andesite is not particularly abundant, so this factor was probably of relatively minor importance.

Volcanic production rates for episodes 4 and 5 are higher by a factor of 1.6-3.3 relative to rates calculated for similar intervals by *Sherrod and Smith* [this issue]. The differences in rate are probably due to differing assumptions about the amount of rock in grabens, and to the fact that their study area spans parts of the arc where grabens may not be present. *Sherrod and Smith* [this issue] do not present cross sections, but judging from cross sections near Mount Jefferson of *Sherrod* [1986] and Sherrod's Figure 7 of *Priest et al.* [1987*a*], they assumed a combined thickness of 460-1200 m of episode 4 and 5 rock with about 30-150 m of episode 5 rock in the main graben structure, excluding stratocones. I inferred thicknesses of 240-700 m and 60-300 m for episodes 4 and 5, respectively, in the same area (Figure 5). Integrating cross section B-B′ (Figure 5) and dividing by the arc width yields average thicknesses for episode 4 and 5 rocks of 450 and 280 m, respectively. The inferred extent of the thickest part of the episode 4 and 5 rock in the graben is apparently the source of the rate discrepancy. *Sherrod* [1986, p. 72] shows the rock thinning very quickly from the crest of the range to the east, whereas I infer from new drill hole data near Green Ridge (drill hole 82-3, Table 1 [*Priest et al.*, 1989]) that the intragraben rocks are quite thick on the east. This factor and my assumption that similar thicknesses apply farther south in the study area are apparently the most important reason for the discrepancy with *Sherrod and Smith* [this issue].

A contributing factor is the large volume of silicic volcanic rock (84.5 km^3) included in episode 5 that *Sherrod and Smith* [this issue] apparently assigned to episode 4. This silicic rock is exposed in the south central part of the study area (silicic highland of Figure 6), where it is locally quite thick. For example, an age of 0.15 Ma was obtained at a depth of 554 m in a hole drilled almost entirely in silicic volcanic rock below the base of the South Sister (Figure 6; Table 3; unpublished lithologic log of G.L. Black [1989]). There are some reversely polarized outcrops of silicic rock at high elevations in adjacent areas (D.R. Sherrod, written communication, 1990), so inclusion of all of this rock in episode 5 may be unwarranted. Excluding it would decrease the episode 5 rate by 9.6%.

Differences in volume calculations for the major stratocones in the area is not likely to be a significant source of error in the total volcanic production rate. Stratocones account for only 8.3% of the volume of episode 5 rock in the area.

The potential errors in volcanic rate calculations are so large that modest or even substantial differences from one worker's calculation to another should not be given too much emphasis. This observation applies particularly to absolute rates, which are highly sensitive to the particular method used. The ratio of volcanic rates from one episode to another is probably more reproducible, being less sensitive to changes in method. For example, the volcanic production decreases by a factor of 3.0 from episode 1 to 2 (Table 3), essentially equal to the decrease (factor of 2.6) found by *Verplanck and Duncan* [1987] utilizing thickness rather than volume data.

Discussion

Figure 8 summarizes correlations between changes in volcanic production rate (R_v) in the Cascades and major changes in the angle of convergence (A_c) and orthogonal rate of convergence (V_c). R_v was higher in episode 1 than in any subsequent episode [*Verplanck and Duncan*, 1987], primarily because of the high rate of silicic volcanism (Figure 8). The high R_v may be the result of the high V_c in episode 1 relative to later episodes [*Verplanck and Duncan*, 1987].

The lowest R_v was in episode 2, when the arc was erupting mainly rocks of intermediate composition (Figure 8). R_v then increased somewhat in episodes 3-5, owing to an increase in mafic volcanism (Figure 8). The low R_v in episode 2 may have been caused by decreasing V_c [*Verplanck and Duncan*, 1987], but the increase of R_v in episodes 3-5 occurred when V_c continued to decrease. The increase in R_v of mafic lava flows at 7.4-0 Ma suggests that crustal stress changes, particularly extension, may play a role [*Priest et al.*, 1983].

CHANGES IN CRUSTAL STRESS

Introduction

Nakamura [1977] showed that changes in the principal stress directions can be inferred from dike orientations and structural relationships. According to *Nakamura* [1977, p. 15], "The trends of

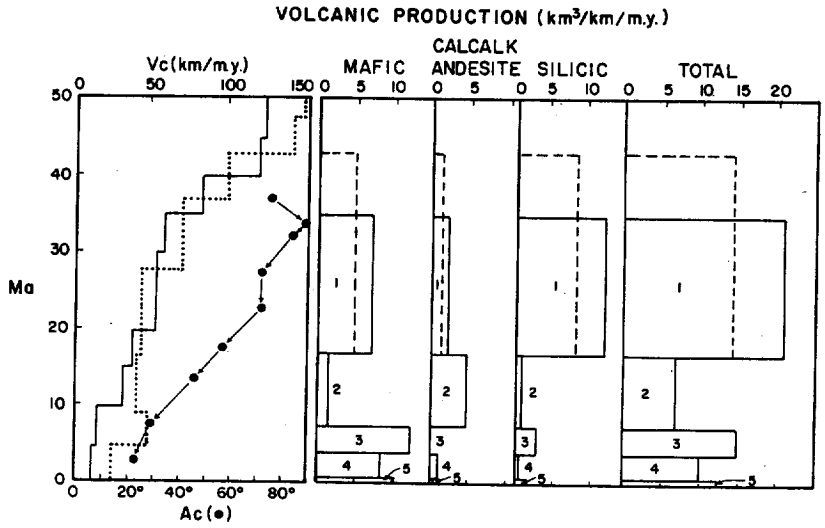

Fig. 8. Comparison of orthogonal convergence rate (V_c), angle between convergence vector and North American plate boundary (A_c), volcanic production rate from Table 3. A_c data points, indicated by the crossed circles, were taken from *Verplanck* [1985] and *Verplanck and Duncan* [1987]; arrows show probable changes between the data points. Solid line represents convergence model of *Verplanck and Duncan* [1987]. Calcalk., calc-alkaline. Note correlation of high volcanic production rate with high V_c during episode 1 and low A_c in episodes 3-5.

dikes (i.e. the trend of the flank crater distribution) may concentrate in a direction of either the maximum compressional [σ_1] or the intermediate stress axis [σ_2] of the regional stress field, or collectively, in a direction normal to the minimum compressional axis [σ_3]." σ_1 is generally horizontal in areas of contractional tectonics, characterized by strike-slip or thrust faults that are not parallel to vertical dikes. In extensional stress regimes, σ_1 is generally vertical, producing normal faults perpendicular to σ_3 but parallel to vertical dikes. The orientation of intrusives and faults in the Cascades is consistent with an extensional stress regime after 7 Ma.

Orientation of Intrusives in the Central Oregon Cascades

Dikes and volcanic vent alignments in the study area are generally aligned northwest in Oligocene and Miocene rocks of the Western Cascades province [*Callaghan and Buddington*, 1938] and north-south in Quaternary rocks of the High Cascades province (*Taylor* [1981]; Sand Mountain area and Devils Lake volcanic center, Figure 6). Statistical studies of dike alignments show that σ_3 has rotated clockwise through time (Figure 9) [*Sherrod and Pickthorn*, 1989].

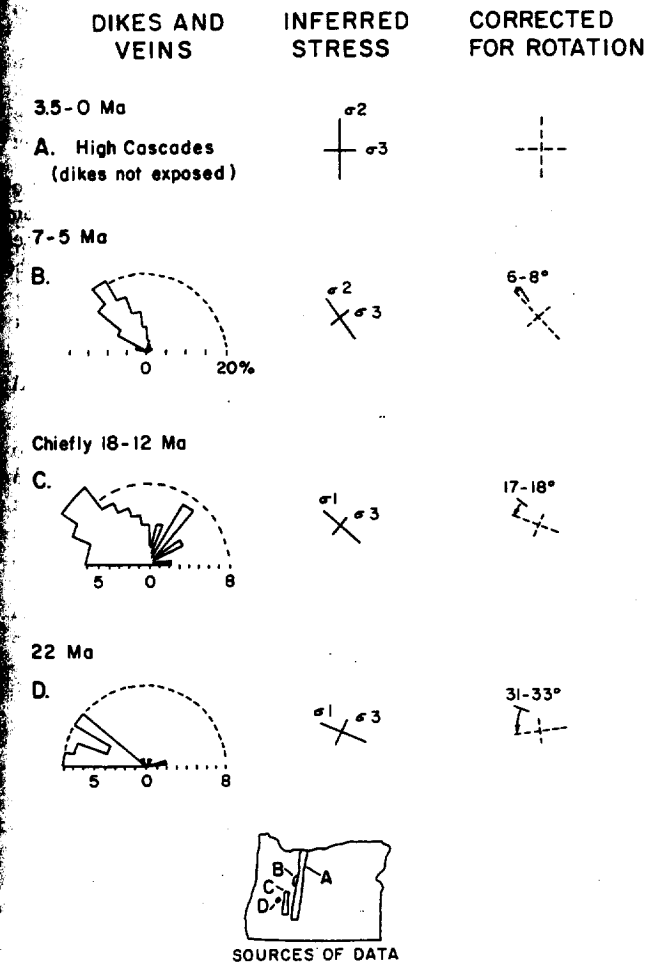

Fig. 9. Dike, vein, and volcanic vent alignment data from the Western Cascades. Figure modified from *Sherrod and Pickthorn* [1989]. (*a*) 3.5-0 Ma, (*b*) 7-5 MA, (*c*) chiefly 18-12 Ma, (*d*) 22 Ma. Data from 43° to 44°N (areas C and D) after dike and vein orientations of *Diller* [1900] and *Sherrod* [1986]. Data of area B from dike orientations of *Avramenko* [1981]. "Inferred stress" shows the orientation of σ_3 and the σ_3-σ_1 or σ_3- σ_2 plane. Rotation of σ_1 to vertical at about 7 Ma is inferred from alignment of normal faults with dike directions after that time. Stress directions for 3.5-0 Ma were inferred from observed north-south alignment of volcanic vents in the High Cascades (area A). "Corrected for rotation" assumes 14°-15° clockwise rotation per 10 m.y. There are no paleomagnetic data specific to these particular rocks. Note the clockwise rotation of σ_3 through time.

Taking into account tectonic rotation based on paleomagnetic data [*Magill and Cox*, 1980; *Grommé et al.*, 1986; *Wells*, this issue], σ_3 rotated from approximately north-south at about 22 Ma to east-west at about 3.5-0 Ma (Figure 9) [*Sherrod and Pickthorn*, 1989]. The orientation of the other principal stress directions can be constrained by consideration of folds and faults.

Folds

Northeast trending middle Miocene folds also occur locally in the Coast Range [*Wells and Peck*, 1961] and areas of the Western Cascades north [*Sherrod and Pickthorn*, 1989; *Beeson et al.*, 1982; *Beeson and Tolan*, this issue] and south [*Sherrod*, 1986] of the study area. It is therefore possible that regional compression affected the Cascades in the middle Miocene. The local nature of the folds suggests rather mild compression.

The only large fold in the study area is the Breitenbush anticline (Figure 6). *Priest et al.* [1987*b*] argued that this structure may be related to local compressive stresses generated in an area of oblique-slip faulting. Regional crustal contraction oriented northwest-southeast could also have caused the fold [*Sherrod*, 1986]. *Sherrod and Conrey* [1988] suggest that this folding probably began after 18 Ma, ending by 12 Ma.

The limbs of the Breitenbush anticline trend from about N20°E on the southwest end of the structure [*Priest et al.*, 1987*b*] to about N45°E at the northeast end [*Sherrod and Conrey*, 1988], so crustal contraction would be parallel to N70°-45°W. Correcting for tectonic rotation [*Wells*, this issue], the contraction was parallel to N85°-57°W in episode 2.

Normal Faults

Northwest trending normal faults of the Tumalo Fault Zone (TFZ, Figure 6) cut Quaternary rocks [*Peterson et al.*, 1976] as young as 300 ka [*Sarna-Wojcicki et al.*, 1987] and merge southeast of the study area with subparallel vent alignments on the flank of Newberry volcano. These faults are on the back side of the arc and may be influenced by preexisting zones of weakness associated with the adjacent Basin and Range or with the thermal anomaly from Newberry volcano [*Priest et al.*, 1983].

North-northwest to north-south trending normal faults active at 5-4 Ma form the boundaries of a graben filled with episode 4 and 5 volcanic rocks [*Taylor*, 1981; *Priest et al.*, 1983, 1988; *Black et al.*, 1987; *Priest*, 1989] (Figures 4-6). Faults of similar age probably lie within the graben, controlling some northerly alignments of Quaternary vents [*Taylor*, 1981]. These buried faults may have continued to be active at 2.4-1.7 Ma and may have significant offsets [*Priest et al.*, 1988; *Priest*, 1989].

Small-displacement, northwest trending normal faults north of Pigeon Prairie (Figure 6) cut basal episode 3 tuff [*Priest et al.*, 1987*b*] but are intruded by a dike that feeds an overlying lava flow time correlative to a lava flow dated at 6.3 Ma [*Priest and Woller*, 1983*b*]. The faults are therefore probably about 7 m.y. old, younger than the beginning of episode 3 (7.4 Ma) but older than 6.3 Ma.

Normal faults have thus changed orientation from northwest at 7 Ma to north-northwest or north-south at 5-0 Ma. Parallelism of the 7-5 Ma faults with contemporaneous dikes and the 5-0 Ma faults with vent alignments (Figure 9) suggests that σ_1 was oriented approximately vertical at 7-0 Ma.

Oblique-Slip Faults

The north-south trending Cougar Reservoir Fault Zone is located spatially and temporally at the transition between the episode 2 and episode 3 volcanic fronts (CRFZ, Figure 6; *Priest and Woller* [1983*a*]). The fault zone is not parallel to the northwest trend of contemporaneous dikes (Figure 9) and has some splinter faults with low-angle slickensides [*Priest and Woller*, 1983*a*]. These features suggest that σ_1 was not vertical at the transition from episode 2 to 3.

The Hoover Fault Zone (HFZ) and an unnamed fault to the west bound a north-northwest tilted block of episode 1 rock within the Breitenbush anticline (Figure 6). The HFZ affects rocks 18 Ma and older, but the age of tilting of the episode 1 rocks on the west side of the fault appears to be older than about 25 Ma (Figure 5) [*Priest et al.*, 1987*b*; *Priest*, 1989]. The HFZ therefore probably had Oligocene and Miocene activity, contemporaneous with both the episode 1 and 2 arcs. The northeast trending HFZ is nearly perpendicular to the predominate trend of contemporaneous dikes (Figure 9) and is associated with numerous shear zones having low-angle slickensides [*Priest et al.*, 1987*b*]. These features suggest that σ_1 was not vertical during episode 1.

Discussion

Aside from possible mild east-west to west-northwest crustal contraction in the middle Miocene, there is no evidence that σ_1 was ever large enough to cause major folding and thrust faulting in the arc. The relationship of dikes to faults suggests that σ_1 rotated from subhorizontal to vertical at about 7 Ma, a few million years after a significant decrease in orthogonal convergence rate (V_c, Figure 10). The arc was therefore probably in an extensional stress regime at 7-0 Ma and only weakly compressional prior to that time.

The minimum compressive stress direction rotated progressively from approximately north-south at 22 Ma to approximately east-west at 4-0 Ma. Clockwise rotation of σ_3 appears to correlate with progressive lowering of V_c, a decreasing angle of convergence (A_c, Figure 10), and growth of the North American plate (NAP)-Pacific plate (PP) transform boundary at the expense of the Juan de Fuca plate (JDFP)-NAP boundary [i.e., *Atwater*, 1970]. Decreasing V_c and A_c probably decreased the influence of northeast compression between the JDFP and NAP, allowing north-south compression at the PP-NAP boundary [*Zoback and Zoback*, 1980; *Spence*, 1989] to increasingly affect stress in the Cascades. The stress regime of the PP-NAP boundary and related stress regimes in the Basin and Range [i.e., *Atwater*, 1970; *Zoback and Zoback*, 1980] therefore increasingly dominated the Cascades from episode 1, when convergence was nearly east-west and rapid, to episodes 3-5, when convergence was slow and highly oblique. At 3.5-0 Ma, extension was approximately east-west, subparallel to that of the Basin and Range province (Figure 10) and perpendicular to the convergent boundary (Figure 1).

The increase of the rollback velocity of the Juan de Fuca plate at 4 Ma may have caused extension perpendicular to the convergent boundary [*Rogers*, 1985] as well as the uplift in the Western Cascades province. I speculate that vigorous circulation of material into the mantle wedge accommodating the increased rollback may have caused the uplift. Increased heat flow or some other factor related directly or indirectly to the flow of mantle material may have caused the uplift. Perhaps the anomalously high surface heat flow and associated gravity anomaly in the eastern part of the Western Cascades physiographic province [*Blackwell et al.*, 1982; *Blackwell et al.*, this issue] is related in some way to this increased back circulation into the mantle wedge.

VOLCANIC ARC MIGRATION

Introduction

Existence of an extinct volcanic mountain range oceanward of the currently active volcanic arc (Figure 4) is proof that eastward arc migration has occurred. Examination of causative processes responsible for volcanic front migration may offer clues to the plate tectonic history.

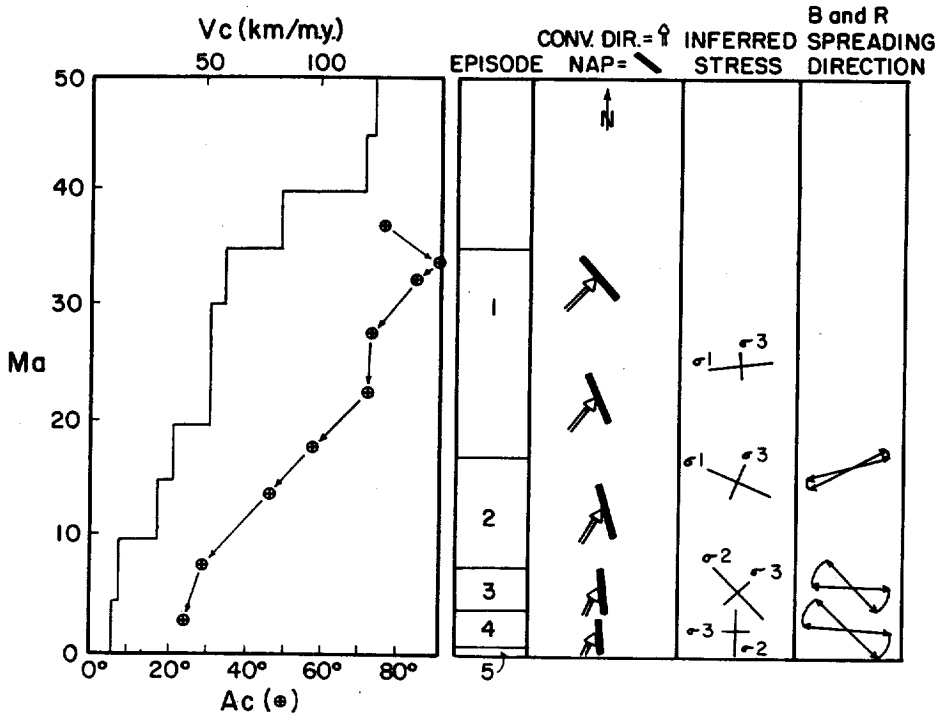

Fig. 10. Comparison of V_c and A_c of Figure 8 to contemporaneous Basin and Range (B&R) spreading directions and principal horizontal stress directions inferred from orientations of Cascade dikes, veins, and volcanic vent alignments as in Figure 9. Double lines with arrows represent the direction of convergence relative to the North American plate (NAP) margin (solid line with no arrows). Normal arrows represent the directions of Basin and Range extension inferred from *Zoback and Thompson* [1978] and *Zoback et al.* [1981]. A_c and orientations of the NAP taken from Verplanck [1985] and *Verplanck and Duncan* [1987]. Note (1) alignment of σ_1 with convergence direction in episode 1; (2) rotation of σ_1 to vertical orientation after marked decrease in V_c at about 10 Ma; and (3) crude alignment of σ_3 with Basin and Range spreading direction in episodes 4 and 5.

Location of Volcanic Fronts

Volcanic fronts for each episode (Figure 11) were placed at the oceanward limit of dense clusters of volcanic vents, near-vent volcanic rocks, or subvolcanic intrusions that appear to mark vent areas. The orientations and locations of volcanic fronts shown in Figure 11 have not been modified for the possible effects of paleomagnetic rotation [i.e., *Magill and Cox*, 1980; *Grommé et al.*, 1986; *Wells*, this issue]. *Wells* [this issue] postulated that Basin and Range extension caused 20° of clockwise block rotation in the western Oregon since the Oligocene, speculating that the mapped volcanic fronts were rifted westward from the active volcanic front. No attempt was made to correct the location of mapped volcanic fronts for rotation inferred from this speculative model.

Location of volcanic fronts for episodes 3, 4, and 5 was relatively easy, owing to good preservation of near-vent volcanic rocks. Location of the volcanic front for episode 2 is highly uncertain, owing to extensive erosion. Figure 11 indicates the probable limits of the uncertainty for the locations of the volcanic front of episode 2. The episode 1 volcanic front is marked by a line of basaltic intrusions and locally thick accumulations of mafic lava flows on the east side of the Willamette Valley (Figure 4).

Isotopic age data near the volcanic fronts of episodes 1-4 [*Walker and Duncan*, 1989] suggest that the front locations shown here are most representative of the beginning of each episode. For example, intrusions with isotopic ages at the episode 1 volcanic front are 35-30 m.y. old [*Lux*, 1982].

The volcanic front has migrated toward the east (Figure 11), but available map data are not detailed enough to recognize whether the migration was continuous or episodic. The average rate of migration is about 2.4 km/m.y. since 30-35 Ma, based on distances between volcanic fronts. Given about 36-41 km of accretion during the same time interval [*Peterson et al.*, 1986], the arc-trench gap has increased at a rate of 3.4-3.8 km/m.y.

Discussion

A number of workers have noted the common occurrence of an extinct volcanic arc outboard from the active arc [e.g., *Dickinson*, 1973; *Gill*, 1981]. Arc-trench gap increases at a mean rate of 1 km/m.y. worldwide [*Dickinson*, 1973]. The following models could individually or in combination explain volcanic arc migration (Figure 12): (1) Change in location of melting above the slab; progressive increase in the depth of melt generation from cooling the mantle wedge [*James*, 1971]; slowing convergence rate narrows the zone of melt generation by decreasing inflow of volatiles and asthenospheric mantle into the wedge [*Taylor*, this issue], (2) Changes in shallow slab dip; progressive decrease of the dip of the slab in the 0-100 km depth range, perhaps by erosion or heating of the lithosphere of the overriding plate [*Jarrard*, 1986], or by lithospheric extension, and (3) Lateral translation of slab; progressive lateral shift of the slab at >100 km depth relative to a fixed point on the overriding plate.

The first method achieves arc migration by moving the zone of melting downdip or laterally relative to a slab of fixed dip. The other models assume that the volcanic front is always about 100-125 km above the slab [*Gill*, 1981; *Jarrard*, 1986]. Arc migration is then achieved by moving the part of the slab at 100-125 km landward by changing the dip at 0-100 km or by rolling the slab back laterally through the mantle at an absolute velocity slower than that of the continental plate.

Slab rollback is caused by vertical sinking of oceanic lithosphere into the mantle [*Dewey*, 1980]. According to *Rogers* [1985, p. 497], for young (<50 Ma) buoyant oceanic lithosphere like that present beneath the Cascades, "the point of action of the rollback vector...is...at the knee bend [of the slab]." The knee bend is probably caused by the basalt-eclogite transition at 60-100 km depth [*Grow and Bowin*, 1975; *Ahrens and Schubert*, 1975].

Unless the Cascade arc is somehow unique among subduction-related arcs worldwide, slab depth below the volcanic front has probably always conformed to the depth of 100-125 km noted by *Gill* [1981] and *Jarrard* [1986] in other arcs. Models 2 and 3 above are therefore probably more likely explanations for the volcanic arc migration.

The previously mentioned paleomagnetic rotation model of *Wells* [this issue] may offer support for model 2. If volcanic fronts in the Western Cascades province were progressively rifted westward by extension in the hotter, weaker lithosphere of the arc and back arc, then a progressively thinned continental lithosphere would be produced in front of the arc. This thinned lithosphere might in fact lower slab dip at 0-100 km, moving the 100-125 km depth contour on the slab eastward.

However, comparison of the various front locations shown by *Wells* [this issue] and this paper (Figure 13) casts some doubt on the accuracy of his data base for front locations. *Wells'* [this issue] pre-Pliocene volcanic front locations do not closely correspond to pre-Pliocene fronts mapped here (Figure 13). Within the study area *Wells* [this issue] shows clockwise rotations relative to the 5-0 Ma volcanic front of 12° and 17° for the 35-18 Ma and 16-10 Ma fronts, respectively (Figure 13). Smaller rotation

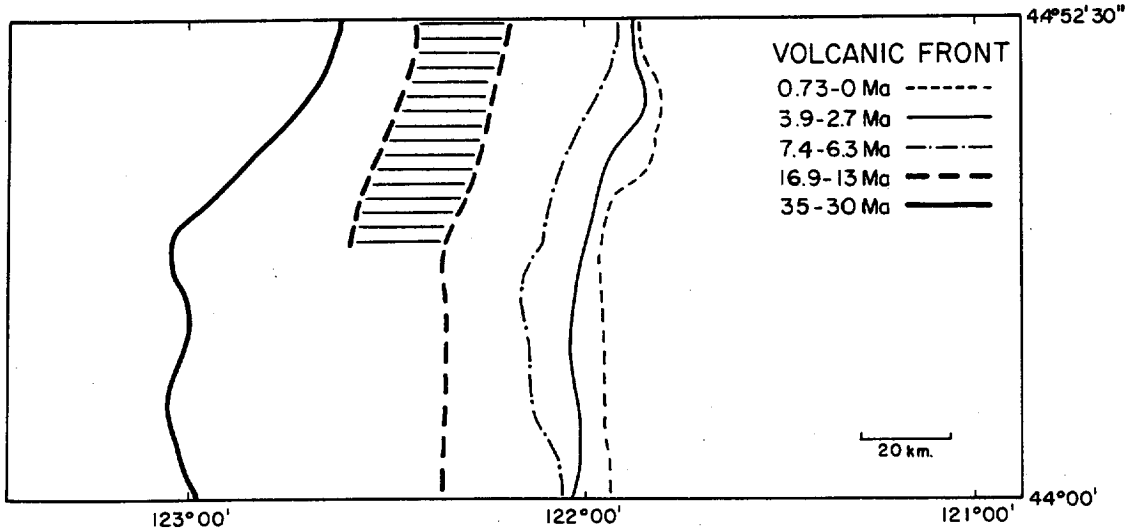

Fig. 11. Map showing inferred volcanic fronts for various times. The two lines shown for 16.9-13 Ma indicate the limits of uncertainty in the location. Note the continuous eastward migration of the volcanic front.

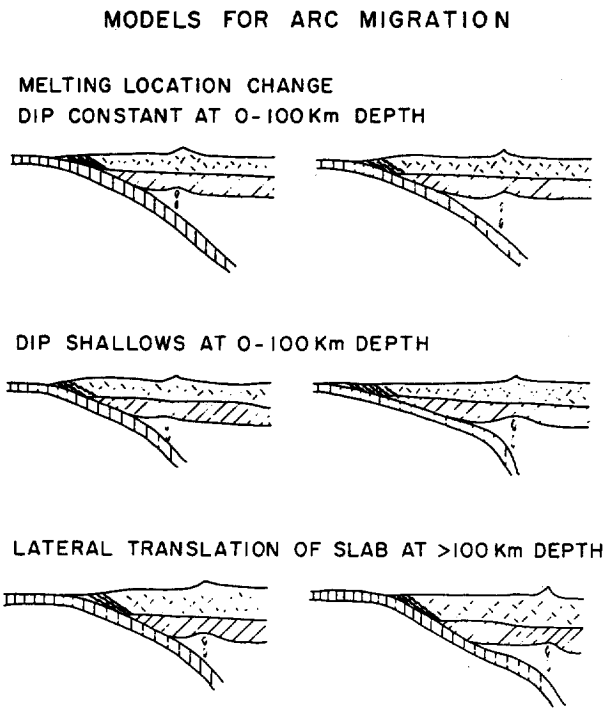

Fig. 12. Cartoons showing three different ways for the volcanic front to migrate landward. Cartoons are not drawn to scale. Vertical lined pattern indicates oceanic crust; herringbone pattern indicates continental crust; slanted lines indicate mantle lithosphere. The last model achieves lateral translation of the deep (>100 km depth) slab relative to the overriding plate by an increase in the velocity of the overriding plate relative to the free rollback velocity of the subducted plate. Other models are self explanatory and are discussed also in the text.

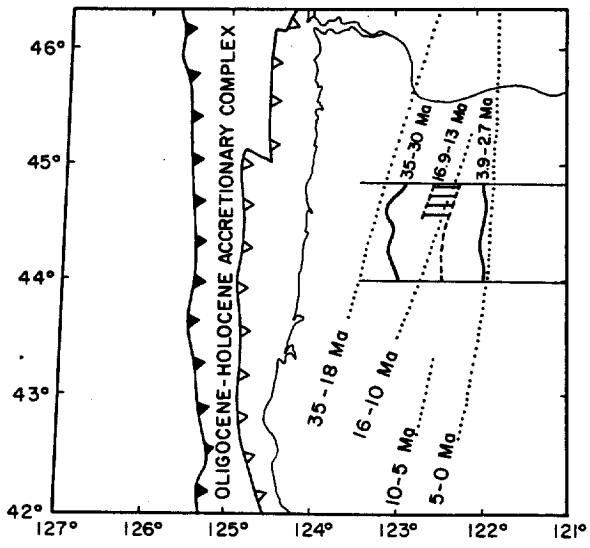

Fig. 13. Cascadia subduction zone (solid saw teeth) and the boundary of the Oligocene-Holocene accretionary complex with older rocks (open saw teeth) from map of *Peterson et al.* [1986]. Dotted lines are volcanic fronts from *Wells* [this issue]. Heavy solid and dashed lines in the study area (rectangular box) are corresponding volcanic fronts of this paper. Note (1) greater clockwise rotation of *Wells'* [this issue] 16-10 Ma front relative to his 35-18 Ma front, (2) lack of correspondence of pre-Pliocene fronts of Wells [this issue] with mapped fronts in the study area, and (3) approximate parallelism of mapped volcanic fronts in the study area with each other and with the Oligocene and Holocene plate boundaries.

for the older front does not fit his progressive extension model.

Subduction-related volcanic arcs world wide are approximately parallel to the convergent plate boundary. This is also true for the 0.7-0 Ma arc in the Cascades (Figure 13), so it is logical to assume that older fronts were also subparallel to the boundary. The Oligocene convergent boundary, as reconstructed from the width of accretionary complex (Figure 13), is subparallel to the present convergent boundary and to all mapped volcanic fronts of this paper, showing a distinct lack of parallelism to the 35-18 Ma front shown by *Wells* [this issue] (Figure 13). These observations cast further doubt on both the model and the data base utilized by *Wells* [this issue] to infer rotation of the volcanic fronts.

The following discussion of slab dip reinforces the interpretation that eastward migration of the volcanic front is chiefly a function of slab dip, if the depth to the slab below the front has remained constant.

CHANGES IN THE DIP OF THE SUBDUCTED SLAB

Estimation of Subducted Slab Configuration

The current location of the upper surface of the subducted slab was inferred on the cross section of Figure 14 by assuming that the volcanic front is about 100-125 km above the slab [*Gill*, 1981] and that the narrow width of the volcanic arc is indicative of a slab dip beneath the arc of about 70° [*Guffanti and Weaver*, 1988]. A dip of this magnitude is supported by tomographic images of the slab in Washington and northern Oregon [*Rasmussen and Humphreys*, 1988]. Extending the shallow slab dip obtained from seismic reflection data [*Snavely et al.*, 1980; *Keach et al.*, 1989] to the intersection with a deep dip of 70° produces a sharp knee bend in the slab at about 70 km depth (Figure 14). This depth is in the range of depth expected for the basalt-eclogite transition in subduction zones worldwide [*Ahrens and Schubert*, 1975; *Grow and Bowin*, 1975].

Most subducted slabs that are well defined by seismic data are inferred to have downward curving surfaces rather than sharp bends [e.g., *Jarrard*, 1986, p. 223]. Cartoons showing possible slab configurations in the past are therefore drawn with curving profiles (Figure 15). Slab positions in the past were inferred from the following observations in present-day subduction zones:

1. Dip steepens in the depth range 60-100 km [*Jarrard*, 1986] as a result of the basalt/eclogite transition [*Grow and Bowin*, 1975: *Ahrens and Schubert*, 1975].
2. The slab was 100-125 km below volcanic fronts [*Gill*, 1981].
3. The dip of the slab below 100 km has increased through time. This is inferred from progressive decrease in the width of the volcanic arc (Figure 7). Decrease of the width of the arc through time is inferred from the eastward migration of the volcanic front (Figure 11) and from local outcrops of volcanic centers and near-vent rocks mapped on the east side of the arc (i.e., Figure 6) [*Smith*, 1986; *Weidenheim*, 1980; *Hales*, 1975; *Conrey*, 1985; *Yogodzinski*, 1986].
4. Accretion of a sedimentary prism caused oceanward migration of the oceanic trench relative to a fixed point on the overriding plate. Accretion is assumed to have occurred at a decreasing rate as convergence rate decreased for the last 35 m.y. Total accretion varies from 36 to 41 km, averaging about 38 km [*Peterson et al.*, 1986].

Discussion

Assuming that the volcanic front has always been 100-125 km above the slab, it is difficult to draw credible pre-7.4 Ma slab positions without decreasing the slab dip at 0-100 km depth and steepening the dip at >100 km depth (Figure 15). This observation lends support to the arc migration model of *Jarrard* [1986] which requires lowering of the shallow (<100 km depth) slab dip by lithospheric thinning in the overriding plate (Figure 12). The young

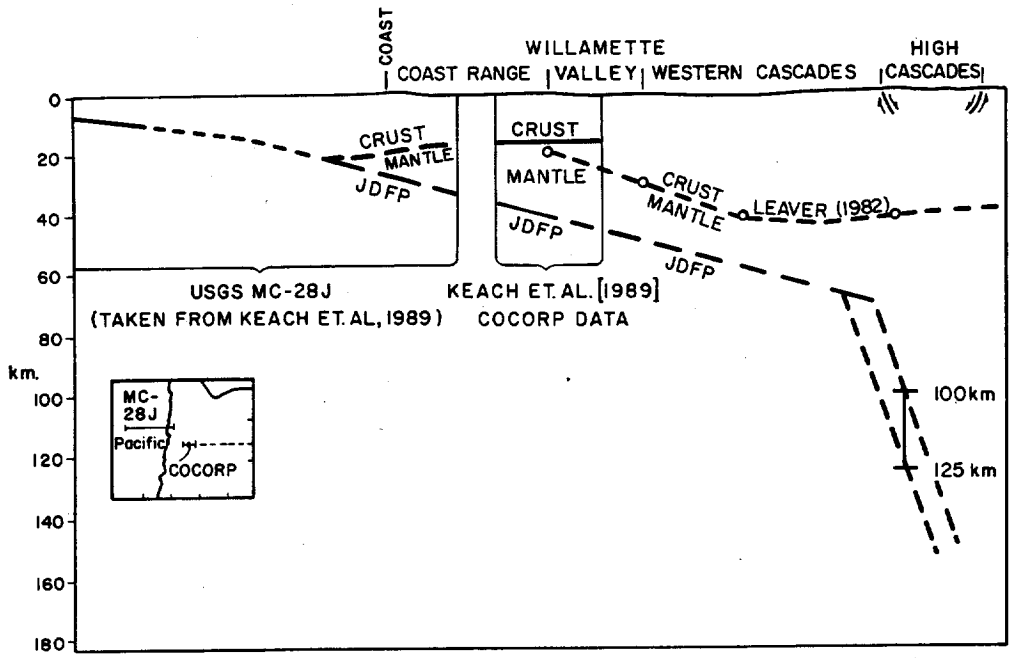

Fig. 14. Regional cross section showing the current crust-mantle-Juan de Fuca plate boundaries. Figure is modified from *Keach et al.* [1989, Figure 8] by (1) adding the crust-mantle boundary of *Leaver* [1982]; (2) assuming a 70° dip for the slab under the High Cascades; (3) assuming that the current volcanic front is about 100-125 km above the slab; and (4) extending the known shallow dip of the slab to meet the 70° dip. USGS MC-28J refers to a Geological Society of America continental margin transect [*Snaveley et al.*, 1980]; JDFP, upper surface of the Juan de Fuca plate.

age of the subducted slab (Figure 15) suggests that the slab, owing to its buoyancy, might in fact conform closely to the shape of the continental lithosphere. Operation of a "suction" force resulting from flow in the mantle wedge [i.e., *Saucier et al.*, 1988] might also tend to pull the slab against the continental lithosphere.

Increasing the dip of the subducted slab behind the volcanic front is the most obvious way of progressively narrowing the arc, but *Taylor* [this issue] favors a different model. He postulates that progressively decreasing convergence rate during the last 35 m.y. would decrease the amount of volatiles carried to great depth and the amount of back circulation of mantle material into the wedge. The zone of melting in the wedge would therefore narrow with time without changes in slab dip.

Alkaline volcanism would be expected if melts were segregated at great depth [e.g., *Green*, 1968]. The *Taylor* [this issue] hypothesis therefore accounts for eruption of the alkaline basalt of the John Day Formation behind the arc in episode 1 but not in later episodes when convergence was slower and shallower melting presumably occurred.

Steepening of the slab behind the volcanic front is favored by the inferred very high (65°-70°) dip of the current subducted slab in the Pacific Northwest [*Guffanti and Weaver*, 1988; *Rasmussen and Humphreys*, 1988]. If the slab dip at >100 km depth were 65°-70° at 35-17 Ma, then the depth to the slab on the landward side of the volcanic arc should have been about 400-500 km. This depth is large relative to the depths to slabs on the back side of other arcs of similar (140 km) width (e.g., compare to *Kuno*, [1966]). Indeed, the model shown by *Taylor* [this issue, Figure 4] requires a constant slab dip at 50-200 km depth of only about 30°-37° for the last 35-40 m.y. Therefore the *Taylor* [this issue] model is not sufficient; progressive steepening of slab dip is also needed to explain arc migration.

The cause of progressive steepening of slab dip behind the volcanic front is not known. Slab dip below 100 km depth may increase owing to (1) large-scale flow within the mantle [i.e., *Jarrard*, 1986], or to (2) decreasing size of the Juan de Fuca plate [*Rasmussen et al.*, 1987]. *Rasmussen et al.* [1987, p. 1379] speculated that "the small area of the Juan de Fuca plate results in only a small amount of local mantle flow and therefore a diminished amount of dynamic support for the descending slab."

Changes in Absolute Plate Motions

Introduction

Rapid changes in absolute velocity of the plates might cause changes in the rate or direction of arc migration (e.g., Figure 12). Absolute velocity changes may also cause deformation events in the overriding plate [e.g., *Pollitz*, 1988; *Rogers*, 1985].

Observations

Relative changes between the westward component of absolute velocity (relative to hot spots) of the overriding plate (V_o) and rollback velocity of the oceanic plate (V_r) in the study area at 35-4 Ma are probably due mainly to changes in V_o. V_r is a function of the buoyancy and thus the age of the subducted part of the slab [e.g., *Oldenburg*, 1975]. The age of the subducted part of the slab at the latitude of the study area has not changed significantly at 35-4 Ma (Figure 15), so V_r has probably not undergone any major changes. V_o of the North American plate (NAP) relative to hot spots has, however, decreased throughout the last 35 m.y. (e.g., Figure 2 of *Morgan* [1983]).

At 4-0 Ma, changes in absolute plate velocity were probably mainly caused by changes in V_r. *Rogers* [1985] argues that V_r of the Juan de Fuca plate increased at about 4 Ma as a result of separation of the buoyant Explorer plate.

Discussion

There is evidence that velocity of volcanic front migration (V_f) in the Cascade volcanic arc in Canada was affected by the increase in V_r at 4-0 Ma. There is no evidence that the NAP changed velocity

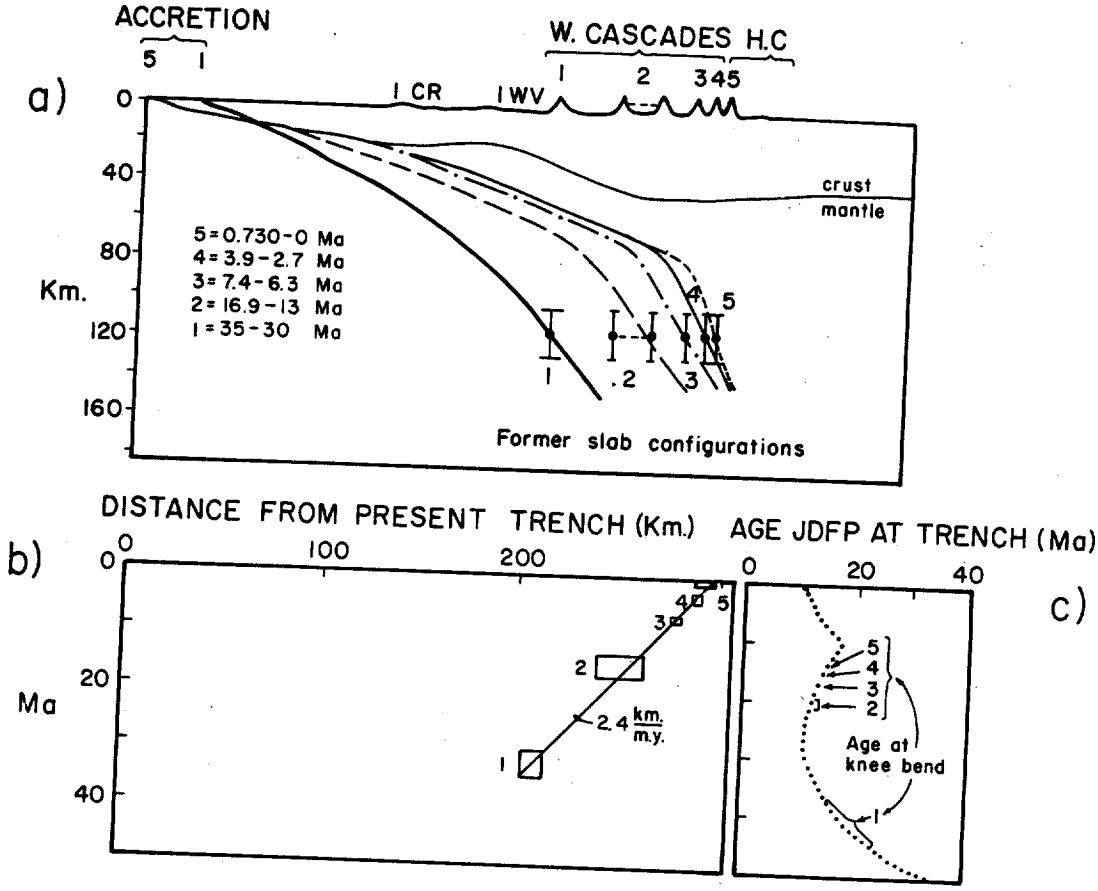

Fig. 15. Regional cross section showing the crust-mantle boundary and the subducted slab. Modified from Figure 14 by adding speculative reconstructions of the slab positions under the volcanic arc during episodes 1-4 (see text), and, in the east half of the section, the crust-mantle boundary of *Leaver* [1982]. Lower figure shows volcanic front migration in time-distance space. The bars and boxes represent the uncertainty of location of the volcanic front in time and space; straight line through the boxes is the average path with slope of 2.4 km/m.y. Also shown is the age of the slab at the trench from *Verplanck* [1985] with inferred slab age at the knee bend for each volcanic episode.

abruptly at 4 Ma, so if V_f is a function of the V_o/V_r ratio, then an abrupt increase of V_r should have caused either a decrease in landward V_f or oceanward migration of the arc. Oceanward migration of the arc did occur in British Columbia at 4-0 Ma [*Rogers*, 1985] and possibly in Washington (e.g., Figure 1 of *Leeman et al.* [this issue]), but the arc remained stationary or moved eastward in Oregon (Figure 11).

The 4-0 Ma V_f in Oregon implies that V_o there adjusted to the increased V_r, possibly by extension in the NAP. Extension of the NAP in Oregon is supported by evidence of Pliocene and younger extensional faulting in the High Cascades [e.g., *Taylor*, 1981; *Sherrod and Pickthorn*, 1989], and the adjacent Basin and Range [*Donath*, 1962; *Lawrence*, 1976].

Likewise, large amounts of 37-0 Ma arc and back arc extension (200-250 km at 42°N) inferred from paleomagnetic data [*Wells and Heller*, 1988; *Wells*, this issue] suggest that V_o in Oregon has been increased by NAP extension throughout the life of the arc. *Pollitz* [1988] inferred that Basin and Range spreading accelerated and altered direction at 9 Ma in response to a decrease in V_o at the Yellowstone hot spot. Extension rates in the western NAP may therefore actually compensate for V_o decreases in the eastern NAP, thereby reducing any inferred decreases at the leading edge of the NAP. "Suction" effects resulting from corner flow in the mantle wedge [*Saucier et al.*, 1988] may explain the resistance of the leading edge of the continental plate to changes in absolute velocity in the interior. Data on V_o from hot spots are therefore probably not representative of V_o at the volcanic front. V_r is unknown, and NAP extension and V_f data have large uncertainties; therefore the effect of the V_o/V_r ratio on V_f is not known from 35 to 4 Ma.

Conclusions

The volcanic front of the Cascade arc migrated progressively inland between 35 and 0 Ma as the volcanic belt narrowed. Narrowing at 35-7.4 Ma was probably caused primarily by progressive steepening of the slab dip at >100 km depth, possibly enhanced by decreasing downdip extent of the zone of partial melt generation above the slab. The landward migration was probably caused by lowering of the dip of the relatively hot, buoyant slab at 0-100 km depth. Thinning of the overriding plate by extension, heating, and basal erosion may have lowered slab dip at 0-100 km depth. Paleomagnetic rotation data can in part be explained by arc and back arc extension [*Wells*, this issue] which may have contributed to thinning of continental lithosphere.

The ratio of slab rollback velocity to the velocity of the overriding plate may also have played a role in arc migration, at least for the last 4 m.y. The arc in British Columbia and possibly in Washington migrated oceanward from 4 to 0 Ma. The migration may have been in response to an increase of free rollback rate of the Juan de Fuca plate. Extension in central Oregon may have increased the westward component of velocity of the North American plate enough to prevent westward arc migration.

The orientation of vertical dikes and volcanic vent alignments

dicate that from 22 to 0 Ma, σ_3 in the Cascade arc rotated clockwise om approximately north-south to east-west. The relationship of ault and fold orientation to contemporaneous dikes suggests that σ_1 may have rotated from subhorizontal to vertical at 7 Ma. Rotation of σ_1 and σ_3 was likely a response to decreasing influence of east-northeast to northeast compression at the Juan de Fuca plate-North American plate (JDFP-NAP) boundary relative to north-south compression and attendant continental extension produced at the Pacific plate (PP)-NAP transform boundary. The stress rotations may have been caused by decreases in orthogonal convergence rate (V_c), convergence angle, and length of the convergent margin relative to the PP-NAP transform boundary.

The rate of Cascade volcanism was highest at 35-17 Ma, when the velocity of plate convergence was highest. Tholeiitic lava, silicic tuff, and subordinate andesite were the chief eruptive products. Volcanic production, particularly production of mafic and silicic rocks, was lower by a factor of 3 at 16.9-7.5 Ma relative to 35-17 Ma. Decreased crustal extension and convergence rate may have been the cause. Local folding in the middle Miocene suggests that crustal extension was in fact low.

Volcanic production, particularly the production of basalt and basaltic andesite, increased somewhat at 7.4-0 Ma, even though convergence rate continued to decrease. The extensional stress regime inferred from dike and fault data at 7-0 Ma may have improved the opportunity for mafic volcanism, explaining the increase in volcanic production in spite of decreasing convergence rate. I speculate that volcanic production in the Cascades is strongly influenced by upper plate stress regime.

The trend of volcanic vent alignments and dikes indicates that at some time between about 5 and 3.5 Ma the direction of σ_3 shifted to approximately east-west, subparallel to Basin and Range extension. This shift is roughly contemporaneous with (1) an increase in rollback velocity of the subducted slab, (2) continued decreases in convergence rate and angle, (3) formation of arc-parallel grabens in the arc, and (4) uplift of the Western Cascades province. Increase of slab rollback velocity at 4 Ma may have contributed to east-west extension in the arc [*Rogers*, 1985]. I speculate that vigorous circulation of material into the mantle wedge accommodating the increased rollback velocity may have played a role in uplift of the Western Cascades province.

Acknowledgements. This investigation was supported by the U.S. Department of Energy in cooperation with the State of Oregon. I am deeply indebted to George W. Walker and David R. Sherrod of the U.S. Geological Survey (USGS) for providing their unpublished scale 1:250,000 geologic maps of the study area. David R. Sherrod and James G. Smith of the U.S. Geological Survey (USGS), Richard M. Conrey (Washington State University), David D. Blackwell (Southern Methodist University), and Robert Yeats and Robert A. Duncan of Oregon State University (OSU) reviewed the paper. Ray E. Wells (USGS) and Edward M. Taylor (OSU) provided many helpful ideas and criticisms. Gerald L. Black of the Oregon Department of Geology and Mineral Industries provided invaluable help with data base management. He and Neil M. Woller (Rittenhouse, Zeman and Associates) worked with me through years of arduous field work, producing the detailed geologic maps that were essential to unraveling the volcanic stratigraphy in the central Oregon Cascades. Barbara J. Priest drafted most of the figures for the paper.

REFERENCES

Ahrens, T.J., and G. Schubert, Gabbro-eclogite reaction rate and its geophysical significance, *Rev. Geophys., 13*, 383-400, 1975.

Atwater, T., Implications of plate tectonics for the Cenozoic tectonic evolution of western North America, *Geol. Soc. Am. Bull., 81*, 3513-3535, 1970.

Avramenko, W., Volcanism and structure in the vicinity of Echo Mountain, central Oregon Cascade Range, master's thesis, 156 pp., Univ. of Oreg., Eugene, 1981.

Bates, R.L., and J.A. Jackson (Eds.), *Glossary of Geology*, 374 pp., American Geological Institute, Falls Church, Va., 1980.

Beaulieu, J.D., P.W. Hughes, and R.K. Mathiot, Environmental geology of western Linn County, Oregon, *Bull. Oreg. Dep. Geol. and Miner. Ind. 84*, 117 pp., 1974.

Beeson, M.H., and T.L. Tolan, The Columbia River Basalt Group in the Cascade Range: A middle Miocene reference datum for structural analysis, *J. Geophys. Res.*, this issue.

Beeson, M.H., M.R. Moran, J.L. Anderson, and B.F. Vogt, The relationship of the Columbia River Basalt Group to the geothermal potential of the Mount Hood Area, Oregon, Geology and Geothermal Resources of the Mount Hood Area, Oregon, edited by G.R. Priest and B.F. Vogt, *Spec. Pap. Oreg. Dep. Geol. and Miner. Ind. 14*, 43-46, 1982.

Black, G.L., N.M. Woller, and M.L. Ferns, Geologic map of the Crescent Mountain area, Linn County, Oregon, scale 1:62,500, *Geol. Map Ser. GMS-47*, Oreg. Dep. Geol. and Miner. Ind., Portland, 1987.

Blackwell, D.D., R.G. Bowen, D.A. Hull, J.F. Riccio, and J.L. Steele, Heat flow, arc volcanism, and subduction in northern Oregon, *J. Geophys. Res., 87*, 8735-8754, 1982.

Blackwell, D.D., J.L. Steele, M.K. Frohme, C.F. Murphy, G.R. Priest, and G.L. Black, Heat flow in the Oregon Cascade Range and its correlation with regional gravity, Curie point depths, and geology, *J. Geophys. Res.*, this issue.

Callaghan, E., and A.F. Buddington, Metalliferous mineral deposits of the Cascade Range in Oregon, U.S. Geol. Surv. Bull., 893, 141 pp., 1938.

Conrey, R.M., Volcanic stratigraphy of the Deschutes Formation, Green Ridge to Fly Creek, north-central Oregon, master's thesis, 349 pp., Oreg. State Univ., Corvallis, 1985.

Dewey, J.F., Episodicity, sequence, and style at convergent plate boundaries, The Continental Crust and Its Mineral Deposits, edited by D.W. Strangway, *Geol. Assoc. Can. Spec. Pap., 20*, 553-573, 1980.

Dickinson, W.R., Widths of modern arc-trench gaps proportional to past duration of igneous activity in associated magmatic arcs, *J. Geophys. Res., 78*, 3376-3389, 1973.

Diller, J.S., The Bohemia mining region of Western Oregon, with notes on the Blue River mining region and on the structure and age of the Cascade Range, annual report, part 3, pp. 1-36, U.S. Geol. Surv., Reston, Va., 1900.

Donath, R.M., Analysis of basin-range structure, south-central Oregon, *Geol. Soc. Am. Bull., 73*, 1-16, 1962.

Fiebelkorn, R.B., G.W. Walker, N.S. MacLeod, E.H. McKee, and J.G. Smith, Index to K-Ar age determinations for the State of Oregon, *Isochron West, 37*, 3-60, 1983.

Gill, J.B., *Orogenic Andesites and Plate Tectonics*, 390 pp., Springer-Verlag, New York, 1981.

Green, D.H., Origin of basaltic magmas, in *Basalts—The Poldervaart Treatise on Rocks of Basaltic Composition*, vol. 2, pp. 835-862, edited by H.H. Hess and A. Poldervaart, Wiley-Interscience, New York, 1968.

Grommé, C.S., M.E. Beck, Jr., R.E. Wells, and D.C. Engebretson, Paleomagnetism of the Tertiary Clarno Formation of central Oregon and its significance for the tectonic history of the Pacific Northwest, *J. Geophys. Res., 91*, 14,089-14,103, 1986.

Grow, J.A., and C. Bowin, Evidence for high-density crust and mantle beneath the Chile Trench due to the descending lithosphere, *J. Geophys. Res., 80*, 1449-1458, 1975.

Guffanti, M., and C.S. Weaver, Distribution of late Cenozoic volcanic vents in the Cascade Range: volcanic arc segmentation and regional tectonic considerations, *J. Geophys. Res., 93*, 6513-6529, 1988.

Hales, P.O., Geology of the Green Ridge area, Whitewater River quadrangle, Oregon, master's thesis, 90 pp., Oreg. State Univ., Corvallis, 1975.

Hammond, P.E., J.L. Anderson, and K.J. Manning, Guide to the geology of the upper Clackamas and North Santiam Rivers area, northern Oregon Cascade Range, Geologic Field Trips in Western Oregon and Southwestern Washington, edited by K.F. Oles et al., *Bull. Oreg. Dep. Geol. and Miner. Ind. 101*, 133-167, 1980.

Irvine, T.N., and W.R.A. Baragar, A guide to chemical classifications of the common volcanic rocks, *Can. J. Earth Sci., 8*, 523-548, 1971.

James, D.E., Plate tectonic model for the evolution of the central Andes, *Geol. Soc. Am. Bull., 82*, 3325-3346, 1971.

Jarrard, R.D., Relations among subduction parameters, *J. Geophys. Res., 24*, 217-284, 1986.

Keach, W.R., II, J.E. Oliver, L.D. Brown, and S. Kaufman, Cenozoic active margin and shallow Cascades structure: COCORP results from western Oregon, *Geol. Soc. Am. Bull.*, 101, 783-794, 1989.

Kuno, H., Lateral variation of basalt magma type across continental margins and island arcs, *Bull. Volcanol., 29*, 196-221, 1966.

Lawrence, R.D., Strike-slip fault terminates the basin and range province in Oregon, *Geol. Soc. Am. Bull., 87*, 846-850, 1976.

Leaver, D.S., A refraction study of the Oregon Cascades, master's thesis, 67 pp., Univ. of Wash., Seattle, 1982.

Leeman, W.P., D.R. Smith, W. Hildreth, Z. Palacz, and N. Rogers, Com-

positional diversity of late Cenozoic basalts in a transect across the southern Washington Cascades: Implications for subduction zone magmatism, *J. Geophys. Res.*, this issue.

Lux, D.R., K-Ar and ^{40}Ar-^{39}Ar ages of mid-Tertiary volcanic rocks from the Western Cascade Range, Oregon, *Isochron West, 33*, 27-32, 1982.

Magill J.,and A. Cox, Tectonic rotation of the Oregon Western Cascades, *Spec. Pap. Oreg. Dep. Geol. Miner. Ind. 10*, 67 pp, 1982.

McBirney, A.R., Petrochemistry of the Cascade andesite volcanoes, Andesite Conference Guidebook, edited by H.M. Dole, *Bull. Oreg. Dep. Geol. and Miner. Ind. 62*, 101-107, 1968.

McBirney, A.R., J.F. Sutter, H.R. Naslund, K.G. Sutton, and C.M. White, Episodic volcanism in the central Oregon Cascade Range, *Geology, 12*, 585-589, 1974.

Miyashiro, A., Volcanic rock series in island arcs and active continental margins, *Am. J. Sci., 274*, 321-355, 1974.

Morgan, W.J., Hotspot tracks and the early rifting of the Atlantic, *Tectonophysics, 94*, 123-139, 1983.

Nakamura, K., Volcanos as possible indicators of tectonic stress orientation—Principle and proposal, *J. Volcanol. and Geotherm. Res. 2*, 1-16, 1977.

Niem, W.A., N.S. MacLeod, and G.R. Priest, Geology, in *CH_2M-Hill, Superconducting Super Collider Site Proposal, University Site, Oregon*, vol. 3, *Geology and Tunneling*, pp. 3-2 to 3-20, CH_2M-Hill, Corvallis, Oreg., 1987.

Oldenburg, D.W., A physical model for the creation of the lithosphere, *Geophys. J. R. Astron. Soc. 43*, 425-451, 1975.

Orr, W.N., and P.R. Miller, Geologic map of the Stayton NE quadrangle, Oregon, *Geol. Map Ser. GMS-34*, scale 1:24000, *Oreg. Dep. Geol. and Miner. Ind.*, Portland, 1984.

Peck, D.L., A.B. Griggs, H.G. Schlicker, F.G. Wells, and H.M. Dole, Geology of the central and northern parts of the western Cascade Range in Oregon, *U.S. Geol. Surv. Prof. Pap., 449*, 56 pp., 1964.

Peterson, N.V., E.A. Groh, E.M. Taylor, and D.E. Stensland, Geology and mineral resources of Deschutes County, Oregon, *Bull. Oreg. Dep. of Geol. and Miner. Ind. 89*, 66 pp., 1976.

Peterson, C.P., L.D. Kulm, and J.J. Gray, Geologic map of the ocean floor off Oregon and the adjacent continental margin, scale 1:500,000, *Geol. Map Ser. GMS-42, Oreg. Dep. Geol. and Miner. Ind.*, Portland, 1986.

Pollitz, F.F., Episodic North America and Pacific plate motions, *Tectonics, 7*, 711-726, 1988.

Power, S.G., C.W. Field, R.L. Armstrong, and J.E. Harakal, K-Ar ages of plutonism and mineralization, Western Cascades, Oregon and southern Washington, *Isochron West*, 31, 27-29, 1981.

Priest, G.R., Volcanic and tectonic evolution of the Cascade volcanic arc, 44°00′ to 44°52′30″, Geology, Geophysics, and Tectonic Setting of the Cascade Range, edited by L.J.P. Muffler, D.D. Blackwell, and C.S. Weaver, *U.S. Geol. Surv. Open File Rep. 89-178*, 430-489, 1989.

Priest, G.R., and N.M. Woller, Geology of the Cougar Reservoir area, Lane County, Oregon, Geology and Geothermal Resources of the Central Oregon Cascade Range, edited by G.R. Priest and B.F. Vogt, *Spec. Pap. Oreg. Dep. Geol. and Miner. Ind. 15*, 39-48, 1983*a*.

Priest, G.R., and N.M. Woller, Geology of the Outerson Mountain-Devils Creek area, Marion County, Oregon, Geology and Geothermal Resources of the Central Oregon Cascade Range, edited by G.R. Priest and B.F Vogt, *Spec. Pap. Oreg. Dep. Geol. and Miner. Ind. 15*, 29-38, 1983*b*.

Priest, G.R., N.M. Woller, G.L. Black, and S.H. Evans, Overview of the geology of the central Oregon Cascade Range, Geology and Geothermal Resources of the Central Oregon Cascade Range, edited by G.R. Priest and B.F. Vogt, *Spec. Pap. Oreg. Dep. Geol. and Miner. Ind. 15*, 3-28, 1983.

Priest, G.R., et al., Investigation of the thermal regime and geologic history of the Cascade volcanic arc: First phase of a program for scientific drilling in the Cascade Range, *Open File Rep. O-86-3*, 120 pp., *Oreg. Dep. Geol. and Miner. Ind.*, Portland, 1987*a*.

Priest, G.R., N.M. Woller, and M.L. Ferns, Geologic map of the Breitenbush River area, Linn and Marion Counties, Oregon, scale 1:62,500, *Geol. Map Ser. GMS-46, Oreg. Dep. Geol. and Miner. Ind.*, Portland, 1987*b*.

Priest, G.R., G.L. Black, N.M. Woller, and E.M. Taylor, Geologic map of the McKenzie Bridge quadrangle, Lane County, Oregon, scale 1:62,500, *Geol. Map Ser. GMS-48, Oreg. Dep. Geol. and Miner. Ind.*, Portland, 1988.

Priest, G.R., G.L. Black, J.M. Mattinson, and P.E. Damon, Implications of new isotopic age data from drill holes in the Oregon Cascades (abstract), *EOS Trans. AGU, 70*(43), 1299, 1989.

Rasmussen, J., and E. Humphreys, Tomographic image of the Juan de Fuca plate beneath Washington and western Oregon using teleseismic *P*-wave travel times, *Geophys. Res. Lett., 15*(12), 1417-1420, 1988.

Rasmussen, J.R., E. Humphreys, and K.G. Dueker, *P*-wave velocity structure of the upper mantle beneath Washington and northern Oregon, *EOS Trans. AGU, 68*(44), 1379, 1987.

Riddihough, R., Recent movements of the Juan de Fuca plate system, *J. Geophys. Res., 89*, 6980-6994, 1984.

Robinson, P.T., and G.F. Brem, Guide to geologic field trip between Kimberly and Bend, Oregon, with emphasis on the John Day Formation, Guides to Some Volcanic Terranes in Washington, Idaho, Oregon and Northern California, edited by D.A Johnson, and J. Donnelly-Nolan, *U.S. Geol. Sur. Circ., 838*, 29-40, 1981.

Rogers, G.C., Variation in Cascade volcanism with margin orientation, *Geology, 13*, 495-498, 1985.

Sarna-Wojcicki, A.M., S.D. Morrison, C.E. Meyer, and J.W. Hillhouse, Correlation of upper Cenozoic tephra layers between sediments of the western United States and eastern Pacific Ocean and comparison with biostratigraphic and magnetostratigraphic age data, *Geol. Soc. Am. Bull., 98*, 207-223, 1987.

Saucier, F., E. Humphreys, K. Dueker, and M. Richards, A model of cyclic subduction beneath continents, *EOS Trans. AGU, 69*(44), 1447, 1988.

Sherrod, D.R., Geology, petrology, and volcanic history of a portion of the Cascade Range between latitudes 43°-44°N, central Oregon, U.S.A., doctoral dissertation, 320 pp., Univ. of Calif., Santa Barbara, 1986.

Sherrod, D.R., and R.M. Conrey, Geologic setting of the Breitenbush-Austin Hot Springs area, Cascade Range, north-central Oregon, Geology and Geothermal Resources of the Breitenbush-Austin Hot Springs Area, Clackamas and Marion Counties, Oregon, edited by D.R. Sherrod, *Open File Rep. O-88-5*, pp. 1-14 , *Oreg. Dep. of Geol. and Miner. Ind.*, Portland, 1988.

Sherrod, D.R., and L.B.G. Pickthorn, Some notes on the Neogene structural evolution of the Cascade Range in Oregon, Geology, Geophysics, and Tectonic Setting of the Cascade Range, edited by L.J.P. Muffler, D.D. Blackwell, and C.S. Weaver, *U.S. Geo. Sur. Open File Rep. 89-178*, 351-368, 1989.

Sherrod, D.R., and J.G. Smith, Preliminary map showing upper Eocene to Holocene volcanic and related rocks of the Cascade Range in Oregon, scale 1:500,000, *U.S. Geol. Sur. Open File Rep. 89-14*, 1989.

Sherrod, D.R., and J.G. Smith, Quaternary extrusion rates of the Cascade Range, northwestern United States and southern British Columbia, *J. Geophys. Res.* this issue.

Smith, G.A., Stratigraphy, sedimentology, and petrology of Neogene rocks in the Deschutes Basin, central Oregon, doctoral dissertation, 467 pp, Oreg. State Univ., Corvallis, 1986.

Smith, G.A., The influence of explosive volcanism on fluvial sedimentation: The Deschutes Formation (Neogene) in central Oregon, *J. Sediment. Petrol., 57*(4), 613-629, 1987.

Smith, G.A., L W. Snee, and E.M. Taylor, Stratigraphic, sedimentologic, and petrologic record of late Miocene subsidence of the central Oregon High Cascades, *Geology, 15*, 389-392, 1987.

Smith, J.G., M.S. Swanlan, and A.C. Katcher, An important lower Oligocene welded-tuff marker bed in the Western Cascade Range of southern Oregon (abstract), *Geol. Soc. Am. Abstr. Programs, 12*(3), 153, 1980.

Snavely, P.D., Jr., and H.C. Wagner, Tertiary geologic history of Western Oregon and Washington, *Rep. Invest. Wash. Div. Mines Geol. 22*, 25 pp., 1963.

Snavely, P.D., Jr., H.C. Wagner, and D.L. Lander, Geologic cross section of the central Oregon continental margin, scale 1:250,000, *Map Chart Ser. MC-28J, Geol. Soc. Am.*, Boulder, Colo., 1980.

Spence, W., Stress origins and earthquake potentials in Cascadia, *J. Geophys. Res. 94*, 3076-3088, 1989.

Taylor, E.M., Central High Cascade roadside geology—Bend, Sisters, McKenzie Pass, and Santiam Pass, Oregon, Guides to Some Volcanic Terranes in Washington, Idaho, Oregon, and Northern California, edited by D.A. Johnston and J. Donnelly-Nolan, *U.S. Geol. Sur. Circ., 838*, 55-58, 1981.

Taylor, E.M., Field geology of the northwest quarter of the Broken Top 15′ quadrangle, Deschutes County, Oregon, *Spec. Pap. Oreg. Dep. Geol. Miner. Ind. 21*, 20 pp., 1987.

Taylor, E.M., Volcanic history and tectonic development of the central High Cascade Range, Oregon, *J. Geophys. Res.*, this issue.

Thayer, T.P., Geology of the Salem Hills and the North Santiam River basin, Oregon, *Bull. Oreg. Dep. Geol. and Miner. Ind. 15*, 40 pp., 1939.

Verplanck, E.P, Temporal variations in volume and geochemistry of volcanism in the Western Cascades, Oregon, master's thesis, 115 pp., Oreg. State Univ., Corvallis, 1985.

Verplanck, E.P., and R.A. Duncan, Temporal variations in plate convergence and eruption rates in the Western Cascades, Oregon, *Tectonics*, *6*(2), 197-209, 1987.

Walker, G.W., and R.A. Duncan, Geologic map of the Salem 1° x 2° sheet, Oregon, scale 1:250,000, *U.S. Geol. Sur. Misc. Invest. Map, I-1893*, 1989.

Weidenheim, J.P., Petrography, structure, and stratigraphy of Powell Buttes, Crook County, central Oregon, master's thesis, 95 pp., Oreg. State Univ., Corvallis, 1980.

Wells, F.G., and D.L. Peck, Geologic map of Oregon west of the 121st meridian, scale 1:500,000, *U.S. Geol. Sur. Misc. Invest. Ser. Map, I-325*, 1961.

Wells, R.E., Paleomagnetic rotations and the Cenozoic tectonics of the Cascade arc, Washington, Oregon, and California, *J. Geophys. Res.*, this issue.

Wells, R.E., and P.L. Heller, The relative contribution of accretion, shear, and extension to Cenozoic tectonic rotation in the Pacific Northwest, *Geol. Soc. Am. Bull.*, *100*, 325-338, 1988.

White, C.M., Geology and geochemistry of volcanic rocks in the Detroit area, Western Cascade Range, doctoral dissertation, 178 pp., Univ. of Oreg., Eugene, 1980.

Williams, H., *The Ancient Volcanoes of Oregon*, 2nd ed., 67 pp., Univ. of Oreg. Press, Eugene, 1953.

Woller, N.M., and G.L. Black, Geology of the Waldo Lake-Swift Creek area, Lane and Klamath Counties, Oregon, Geology and Geothermal Resources of the Central Oregon Cascade Range, edited by G.R. Priest and B.F. Vogt, *Spec. Pap. Oreg. Dep. Geol. Miner. Ind. 15*, 57-68, 1983.

Woller, N.M., and G.R. Priest, Geology of the Lookout Point area, Lane County, Oregon, Geology and Geothermal Resources of the Central Oregon Cascade Range, edited by G.R. Priest, and B.F. Vogt, *Spec. Pap. Oreg. Dep. Geol. Miner. Ind. 15*, 49-56. 1983.

Yogodzinski, G.M., The Deschutes Formation-High Cascade transition in the Whitewater River area, Jefferson County, Oregon, master's thesis, 165 pp., Oreg. State Univ., Corvallis, 1986.

Zoback, M.L., and G.A. Thompson, Basin and Range rifting in northern Nevada: Clues from a mid-Miocene rift and its subsequent offsets, *Geology*, *6*, 111-116, 1978.

Zoback, M.L., and M. Zoback, State of stress in the conterminous United States, *J. Geophys. Res.*, *85*, 6113-6156, 1980.

Zoback, M.L., R.E. Anderson, and G.A. Thompson, Cainozoic evolution of the state of stress and style of tectonism of the Basin and Range province of the western United States, *Philos. Trans. R. Soc. London, A-300*, 407-434, 1981.

G.R. Priest, Oregon Department of Geology and Mineral Industries, 910 State Office Building, Portland, OR 97201. Phone: (503) 229-5580. FAX: (503) 229-5639

(Received June 26, 1989;
revised March 28, 1990;
accepted June 19, 1990.)